DOE/JPL-956614-84/01

9950-1801

JCGS

(NASA-CR-175693) INVESTIGATION OF SILICON SURFACE PASSIVATION BY SILICON NITRIDE FILM DEPOSITION Final Report, 1 Sep. 1983 - 31 Aug. 1984 (Joint Center for Graduate Study) 65 p HC A04/MF A01 CSCL 10A G3/44

N85-25938

Unclas 21025

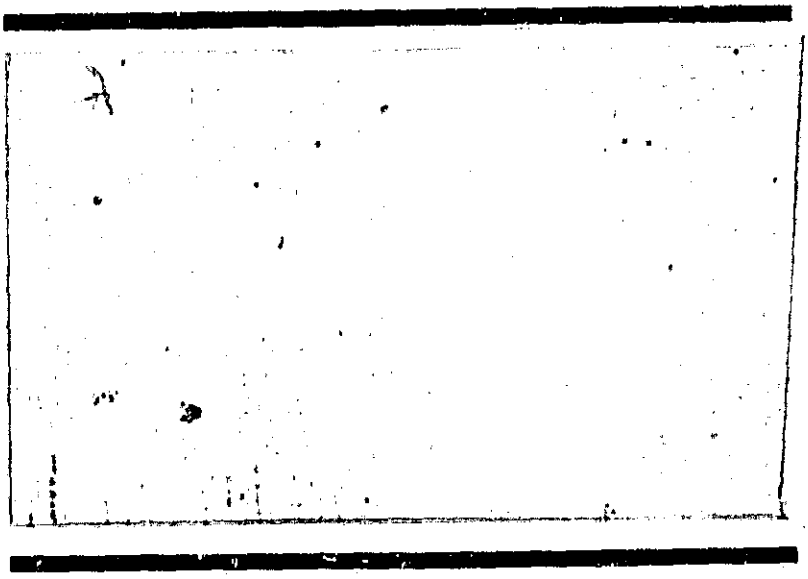

SOLAR ENERGY LABORATORY

JOINT CENTER FOR GRADUATE STUDY

UNIVERSITY OF WASHINGTON / WASHINGTON STATE UNIVERSITY / OREGON STATE UNIVERSITY

INVESTIGATION OF SILICON SURFACE PASSIVATION BY SILICON NITRIDE FILM DEPOSITION

Annual Report

9/1/83 - 8/31/84

JPL Contract No: 956614

September, 1984

By

Professor Larry C. Olsen

Joint Center for Graduate Study
University of Washington
Richland, Washington 99352

This work was performed for the Jet Propulsion Laboratory, California Institute of Technology, and was sponsored by the United States Department of Energy through an agreement with the National Aeronautics and Space Administration.

SUMMARY

Studies of SiN_x-Si interface properties have been conducted for SiN_x films grown on silicon for a range of film growth conditions. Films were grown on silicon wafers having a (100) orientation, and resistivity of 2 Ohm-cm. Two basic cleaning procedures were used: RCA cleaning procedure and a more abbreviated process which omits the RCA peroxide steps. Substrates either had a native oxide or a thin oxide film (20 Å) formed by heat treating the wafer at 500 °C for 20 minutes in oxygen. In addition surfaces were either nitrided or not nitrided. Nitridation involves exposing a surface to a RF plasma and ammonia using 15 W RF power, 70 sccm NH_3 flow, and 270 °C platen temperature. Thus, six initial surface conditions are defined by the various combinations of two chemical cleaning steps (RCA or abbreviated), two oxide films (native or 20 Å), and either nitrided or not.

After surface preparation, SiN_x films were deposited with an RF power of either 13 W or 75 W, and with the platen temperature at 150 °C or 270 °C. After deposition of the films, aluminum gates were deposited on a region of the substrate and the surface state density obtained using high frequency C-V measurements. Effects of heat treatment were studied by annealing the films and depositing additional gates on another region of the substrate, and then conducting C-V measurements. Some key results obtained from this study are: (1) SiN_x film deposition at low RF power (.025 W/cm^2) leads to lower surface state densities; (2) Deposition at 270 °C is preferable for low surface state sensitivities and (3) Nitriding the silicon surface prior to SiN_x deposition results in low surface state densities.

Solar cells without AR coatings were provided by JPL to utilize for investigation of the passivation properties of SiN_x. Two groups of cells were provided: a set of terrestrial standard cells characterized by a base p-type resistivity of 2 Ohm-cm and a junction depth of 0.4 μm; and a group of cells based on 2 Ohm-cm p-type material and a 0.2 μm junction. All cells had Ti/Pd/Ag collector grids. These devices were characterized by photoresponse and current-voltage analyses before and after SiN_x deposition.

Internal photoresponse analyses of the terrestrial standard cells indicated that the surface recombination velocity on the bare front surface (S_F) was typically 3×10^4 cm/sec, while it was $\approx 2 \times 10^4$ cm/sec after SiN_x deposition. I-V analyses indicated the dominant current loss mechanism in these cells is depletion layer recombination with typical parameters for the large voltage mechanism being $n = 1.1$, $J_0 = 10^{-11}$ to 10^{-10} A/cm^2, and an activation energy for J_0 of 0.9 eV. As a result, I-V characteristics of these cells are not sensitive to S_F.

Internal photoresponse studies of the shallow junction cells indicated $S_F \approx 10^5$ cm/sec before and after SiN_x deposition. The PECVD system was in need of repair during the time period these cells were being coated with SiN_x. Thus, the large S_F could have been a result of relatively low quality SiN_x films. On the other hand, the large value of S_F observed for the bare surface suggests that there may be a correlation between S_F and the junction depth--or more importantly, the diffusion process required to achieve the 0.2 μm junction depth.

Preliminary results were obtained for studies involving gated diode device structures. In one case, a decrease in short wavelength photoresponse was observed when a negative potential was applied to the gate of gated N^+/P cell.

TABLE OF CONTENTS

LIST OF TABLES

LIST OF FIGURES

1. INTRODUCTION

The primary objective of the first year effort was to investigate the use of SiN_x grown by plasma enhanced chemical vapor deposition (PECVD) for passivating silicon surfaces. The application of PECVD SiN_x films for passivation of silicon N^+/P or P^+/N solar cells is of particular interest. This program has involved the following areas of investigation:

(i) Establishment of PECVD system and development of procedures for growth of SiN_x;
(ii) Optical characterization of SiN_x films;
(iii) Characterization of the SiN_x/Si interface;
(iv) Surface recombination velocity deduced from photoresponse;
(v) Current-Voltage analyses of silicon N^+/P cells.
(vi) Gated diode device studies.

Significant progress in each of these areas has been accomplished. After purchasing components of a PECVD system, the apparatus was assembled and procedures for growing SiN_x films were developed. Deposition parameters were identified which are appropriate for growing an effective AR coating on an N^+/P cell, and also for achieving a low interface state density on moderately doped silicon. Photoresponse and I-V analyses were carried out for N^+/P cells provided by JPL. These cells were characterized before and after deposition of SiN_x. Surface recombination velocities on the order of 10^4 cm/sec were achieved for the first group of cells, while values on the order of 10^5 cm/sec were determined for a second group of devices. The first group of cells had junction depths of 0.4 μm while the second group had junction depths of 0.2 μm. SiN_x films deposited on cells in the second group were generally of lower quality as indicated by interface state densities determined on witness p-type silicon substrates. As a result, the difference in surface recombination velocities determined for the two cell types is not understood.

Details concerning studies in each of the areas listed above are discussed in the following sections.

2. PECVD SILICON NITRIDE

2.1 PECVD System

A plasma enhanced chemical vapor deposition system (PECVD) was established by modifying a TECHNICS PE-IIA plasma etcher. The Technics system was modified for deposition by installing a platen and gas injection ring. The reactor design is based on the Reinberg approach with two horizontal, parallel capacitor plates 11 inches in diameter and with a one-inch separation. Substrates are supported on the grounded electrode which can be heated to 350°C. Process gases enter the reaction chamber below the grounded electrode, flow radially inward between electrodes and exit through an exhaust at the center. To induce the deposition reaction, a 30 kHz RF glow discharge is established between the electrodes at power densities up to 8000 W/m^2. For SiN_x deposition the reactant gases are silane (SH_4) and ammonia (NH_3). Typial pressures maintained during processing range from 0.2 to 0.8 torr. The system is pumped by an Edwards rotary vane pump. A schematic of the PECVD system is given in Figure 1. A picture of the reaction chamber and control module is shown in Figure 2A, and the platen is shown in Figure 2B. The gas flow control components were purchased from MKS Instruments. A 247/2259 series mass flow controller allows separate or ratioed control of three gases, with a fourth channel in reserve. The flow ranges are 0-150 sccm. Pressure control is achieved with the 252/253 series downstream pressure controller, which reads the output of a capacitance manometer in the vacuum chamber. All plumbing is teflon or stainless steel for the reactive gases.

Silane and ammonia gases were purchased in the highest grades commercially available. A Freon-14/oxygen mixture is used for etching and cleanup, and argon is used as a carrier. All the hazardous gases are housed in a metal enclosure equipped with forced ventilation, temperature sensing, and an alarm and sprinkler system.

SCHEMATIC OF PECVD SYSTEM

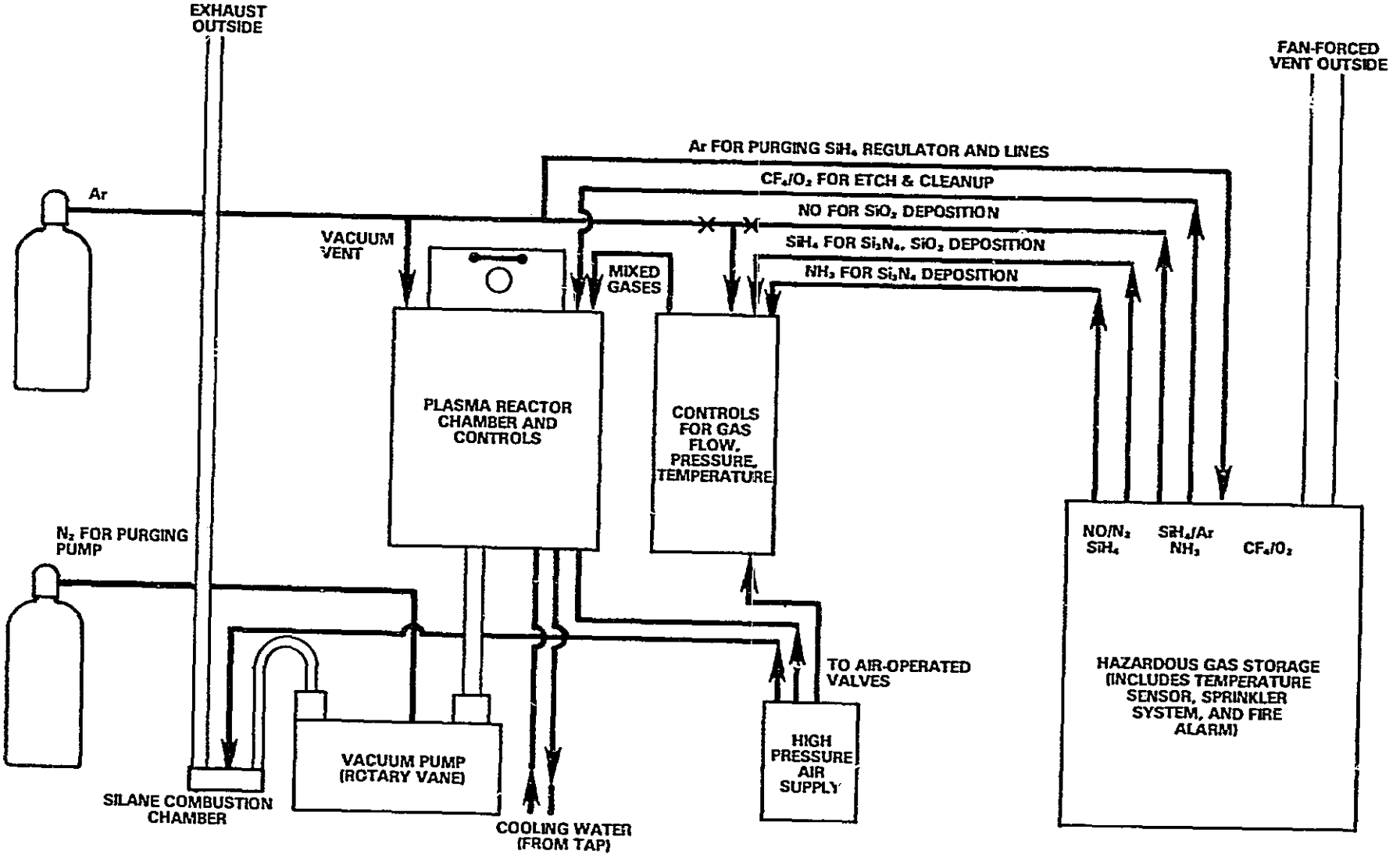

Figure 1

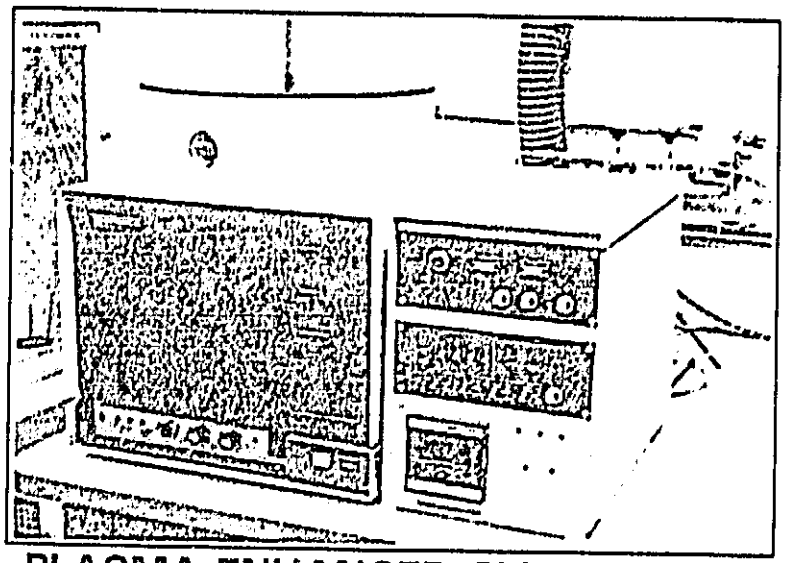

PLASMA ENHANCED CVD SYSTEM

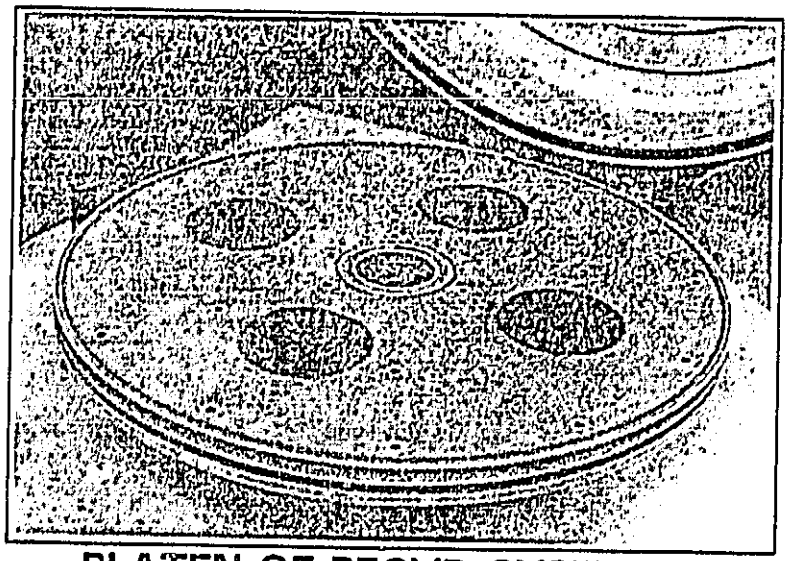

PLATEN OF PECVD SYSTEM

Figure 2. Picture of PECVD System. (A) Deposition Chamber and Control Module, (B) Platen.

2.2 Deposition Parameters

The key process variables for SiN_x film growth are:

- Gas Flow Rates
- NH_3/SiH_4 Gas Flow Ratio
- Platen Temperature
- RF Power
- Chamber Pressure

Process parameters are generally controlled to within one percent during deposition or etching. A typical set of deposition parameters for SiN_x film growth are: SiH_4 flow, 10 sccm; NH_3 flow, 20 sccm; argon flow, 30 sccm; RF power, 1200 W/m^2; platen temperature 270°C; total pressure, 0.48 torr; deposition time, 300 seconds. The resulting SiN_x film would have an index of refraction on the order of 2.0 and a film thickness of 670 A.

3. OPTICAL PROPERTIES OF PECVD SiN_x FILMS

Optical properties of PECVD SiN_x films are of interest since such a film can be used as an AR coating for a silicon cell as well as a passivating surface layer. In this section, the approach used for determining optical constants of AR films on silicon, experimental results for optical constants as a function of growth parameters, estimated values of photocurrent for a single SiN_x AR layer, and for a double AR structure based on the use of two SiN_x films of different composition are discussed.

3.1 Measurement of Optical Constants

Two approaches have been utilized to estimate the optical constants of SiN_x films, namely, ellipsometry and reflectance versus wavelength. PECVD films pose a unique problem since the film thickness is not known. Thickness monitors as used in resistance heated deposition are not compatible with a PECVD process. Reflectance is measured versus wavelength routinely at JCGS. Ellipsometric measurements are done on equipment made available (on a limited basis) by Battelle Northwest Laboratories, Richland, WA.

Ellipsometry, of course, refers to a reflectance measurement which also involves detection of a change in polarization between incident and reflected photons. Ellipsometric measurements on thin films can yield two of three parameters, the index of refraction (N), the extinction coefficient (K) and film thickness. By using optical filters, ellipsometry measurements are conducted at several wavelengths. Since only two of the three variables can be determined, data obtained at 700 nm are analyzed assuming K=0 to determine the film thickness and N at 700 nm. The value of film thickness determined at long wavelengths is then used when analyzing data for $\lambda < 700$ nm. Ellipsometric results for N and K of two SiN_x are shown in Figure 3. Film 84-151 is similar to films used for passivation purposes, and for a single AR coating. Film 84-119 was grown with deposition parameters which yield films containing significant amounts of free silicon.

OPTICAL CONSTANTS OF SiN_x FILMS FROM ELLIPSOMETRY MEASUREMENTS*

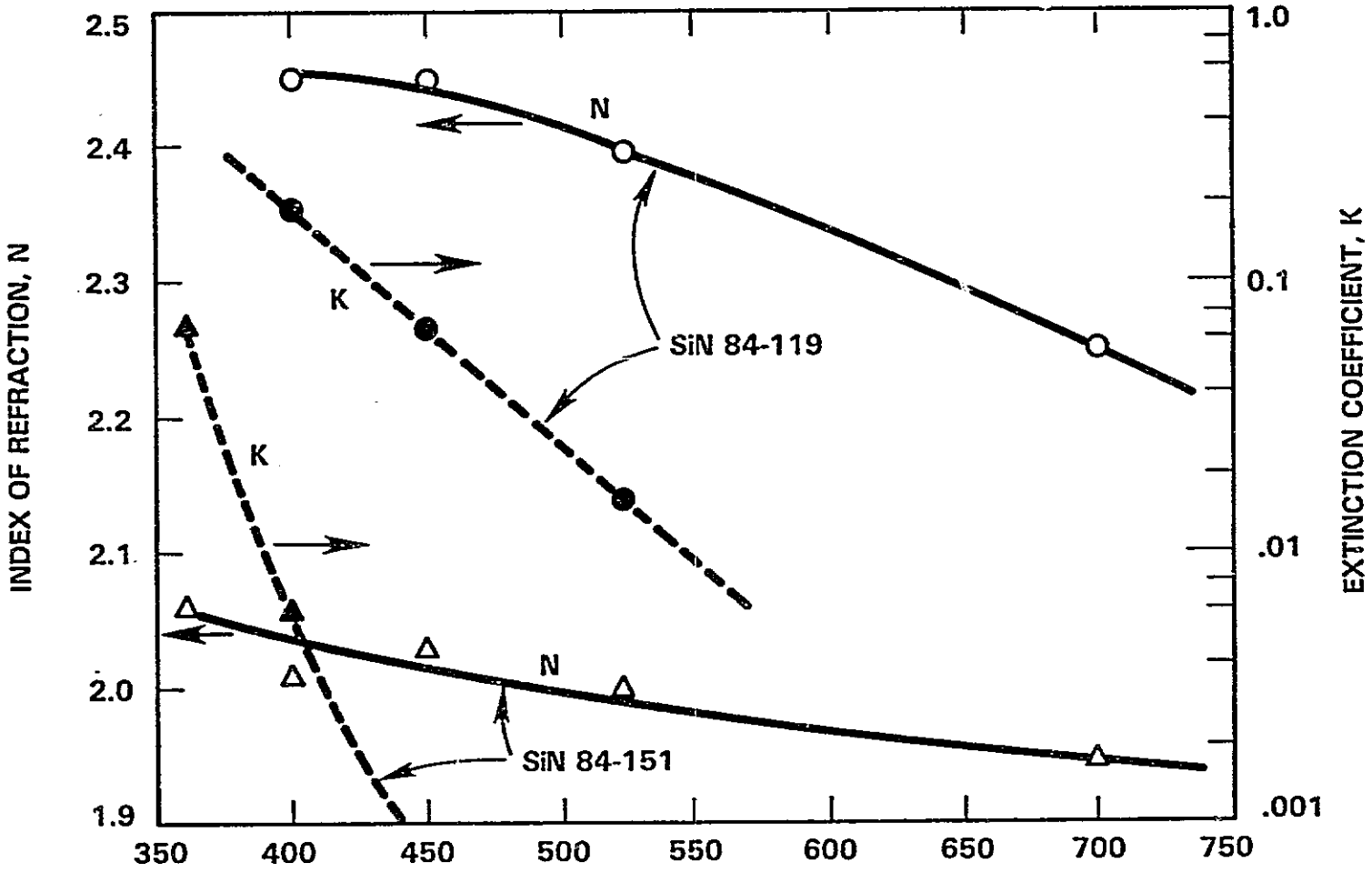

*MEASUREMENTS TAKEN ON EQUIPMENT PROVIDED BY BATTELLE NORTHWEST LABORATORIES

Figure 3

Reflectance measurements are carried out with an approach described by Figure 4. The sample consists of a SiN_x film on a polished silicon substrate. The N and K value of silicon are known.[1] Reflectance is measured from 360 nm to 1200 nm with 20 nm intervals. The measurement is done using the JCGS photoresponse system (briefly described in Section 5). The reflectance data provide information which is only sufficient to determine one parameter of the SiN_x film versus wavelength. However, there are two quantities (N, K) which vary with λ, and the film thickness (d). It is reasonable to assume K = 0 for λ > 600 nm. As a result, we are able to determine d by analyzing the reflectance data at long wavelengths. After obtaining d, an estimate of N vs λ can be obtained based on the assumption that K = 0 for all values of λ . Thus, the following approach is used to analyze reflectance data:

(i) Assume K = 0;

(ii) Determine possible values for N and d which give R for a range of wavelengths;

(iii) Determine N vs λ, assuming K = 0, and by requiring d to be constant.

Values for N vs λ are then determined assuming K = 0. This approach yields values for N to within a few percent unless the films become too absorptive for solar cell applications. To be more specific, consider the results given in Table 1. Film 84-119 and 84-151 are examples of SiN_x films with

TABLE 1

COMPARISON OF OPTICAL CONSTANTS
DETERMINED FROM ELLIPSOMETRY AND ORDINARY REFLECTANCE

SiN_x FILM	GROWTH PARAMETERS	WAVELENGTHS (nm)	ELLIPSOMETRY			REFLECTANCE	
			d	N	K	d	N
84-119	SiH_4 Flow: 10 sccm NH_3 Flow: 5.6 sccm T = 150°C Power = 75 W	400	374	2.45	.188	360	2.35
		450		2.45	.069		2.63
		546		2.39	.016		2.61
		700		2.25	.000		2.42
84-151	SiH_4 Flow: 10 sccm NH_3 Flow: 10 sccm T = 170°C Power = 14 W	360	683	2.06	.071	732	
		400		2.01	.006		1.99
		450		2.03	.000		1.95
		546		2.00	.000		1.93
		700		1.95	.000		1.93

MEASUREMENT OF INDEX OF REFRACTION OF SiN FILMS ON SILICON

- MEASURE R VS. λ
- VALUES OF N_2 VS. λ AND K_2 VS. λ ARE KNOWN
- ASSUME $K_1 \simeq 0$ (PARTICULARLY GOOD APPROXIMATION FOR $\lambda > 500$ nm)
- DETERMINE d AND N_1 VS. λ:
  - —ASSUME N_1 IS CONSTANT OVER 30 nm RANGE FOR $\lambda \sim 600$ nm AND DETERMINE d FROM R VS. λ DATA
  - —THEN DETERMINE N_1 VS. λ

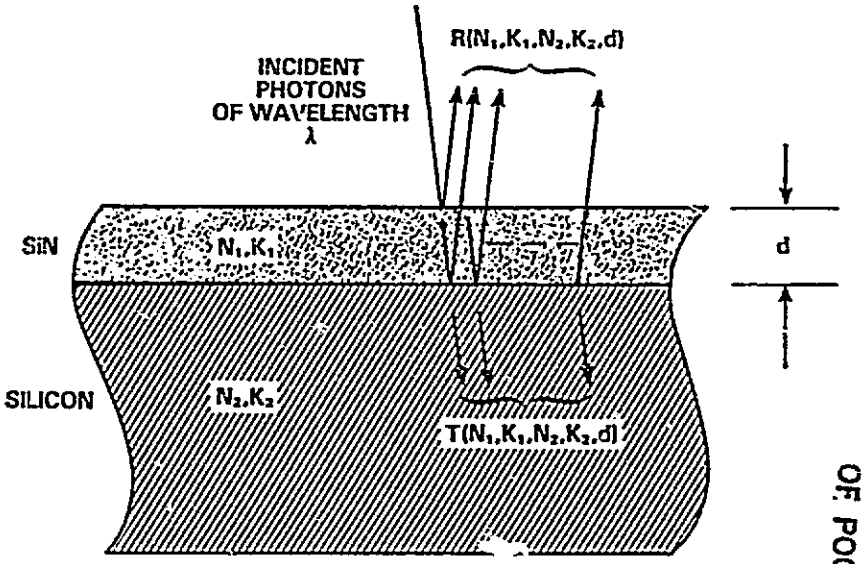

Figure 4

significantly different values for N and d. Results obtained for N and K with ellipsometry are compared to values for N and d determined from ordinary reflectance measurements. The values for d and N agree fairly well. The reflectance measurement is used on a routine basis while ellipsometry is utilized when the equipment can be made available.

3.2 Effect of Deposition Parameters on Optical Properties of SiN_x Films

Investigations of the effect of silane/ammonia ratio, RF power and substrate temperature on the index of refraction have been conducted. Figure 5 shows the range of values determined for N at 500 nm versus SiH_4/NH_3 gas flow ratio, a substrate temperature of 270°C and with RF power set at 1225 W/m^2. If either the power or platen temperature is decreased, the index values will be in the direction of the arrow. These changes in platen temperature and power level favor less Si-N reaction, which results in a film containing more free silicon. Increased power and/or platen temperature leads to lower values of N.

Figure 6 gives results for N vs λ for three films. Consider films SiN 33 and SiN 47. Film SiN 33 was grown under conditions similar to films for which N is plotted in Figure 5. SiN 47 was deposited with a gas flow ratio of SiH_4/NH_3 = .33, but at a larger RF power than SiN 33. As a result the value of N for SiN 47 is larger than SiN 33. Results for SiN 46 indicate the effect of oxygen in SiN_x films, namely, N is lowered.

3.3 Anti-Reflection Coatings Based on SiN_x

It is well established that SiN_x is a good choice for a single AR cell design. It is desirable to utilize films with N near 1.9 and K = 0. Calculated values of active area photocurrent assuming SiN_x films with properties like 84-119, 84-151 and for N = 1.9 and K = 0, are tabulated in Table 2. These calculations are based on a Phoenix, Az, AM1 solar spectrum, a cell internal photoresponse appropriate for silicon cell SiNP2 (See Section 5). In practice, one would expect to deposit films with properties in the range bracketed by SiN 151 and one with N = 1.9, K = 0. Figure 7 shows results of reflectance vs wavelength for a SiN film on silicon which has proper optical properties and thickness for a single AR coating.

SiN_x FILM INDEX OF REFRACTION VS. SILANE/AMMONIA RATIO

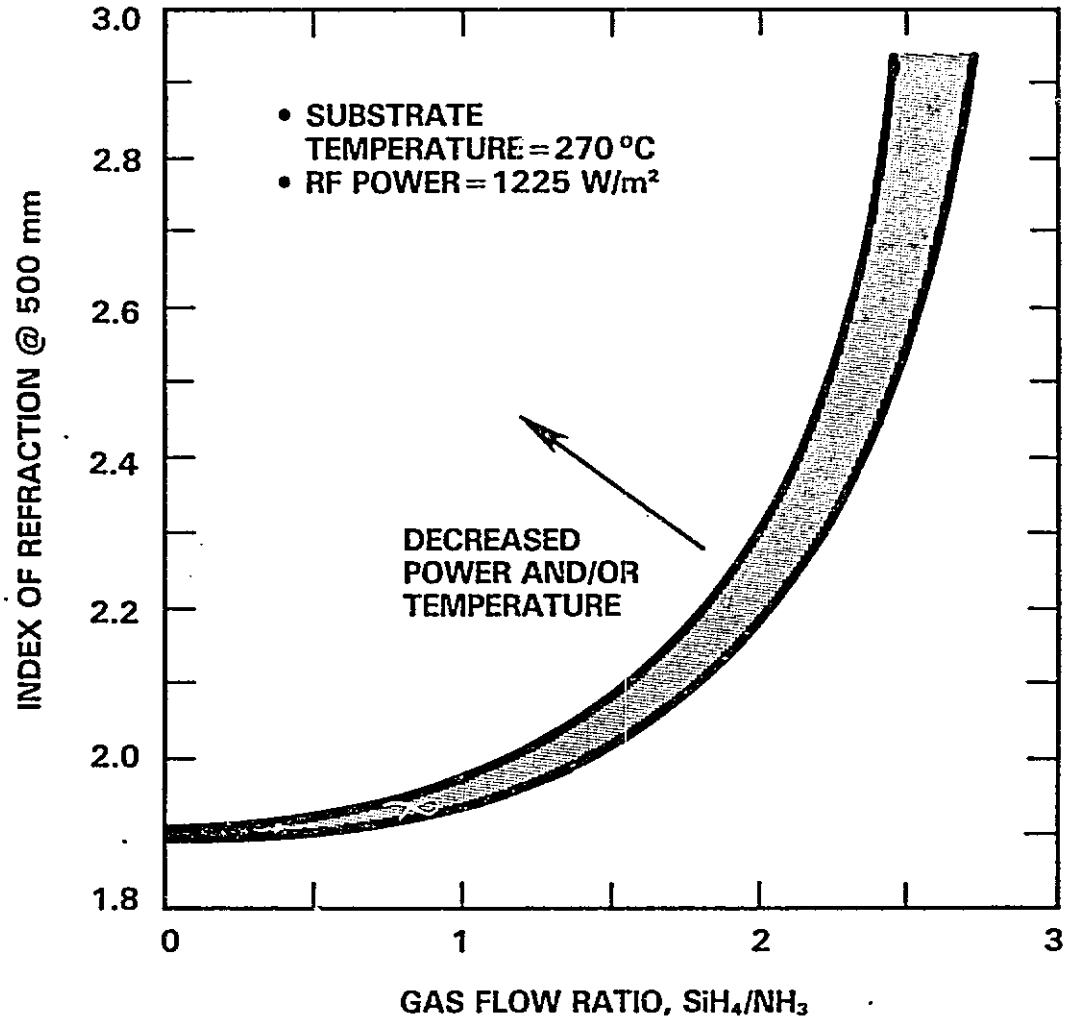

Figure 5

INDEX OF REFRACTION VS. WAVELENGTH

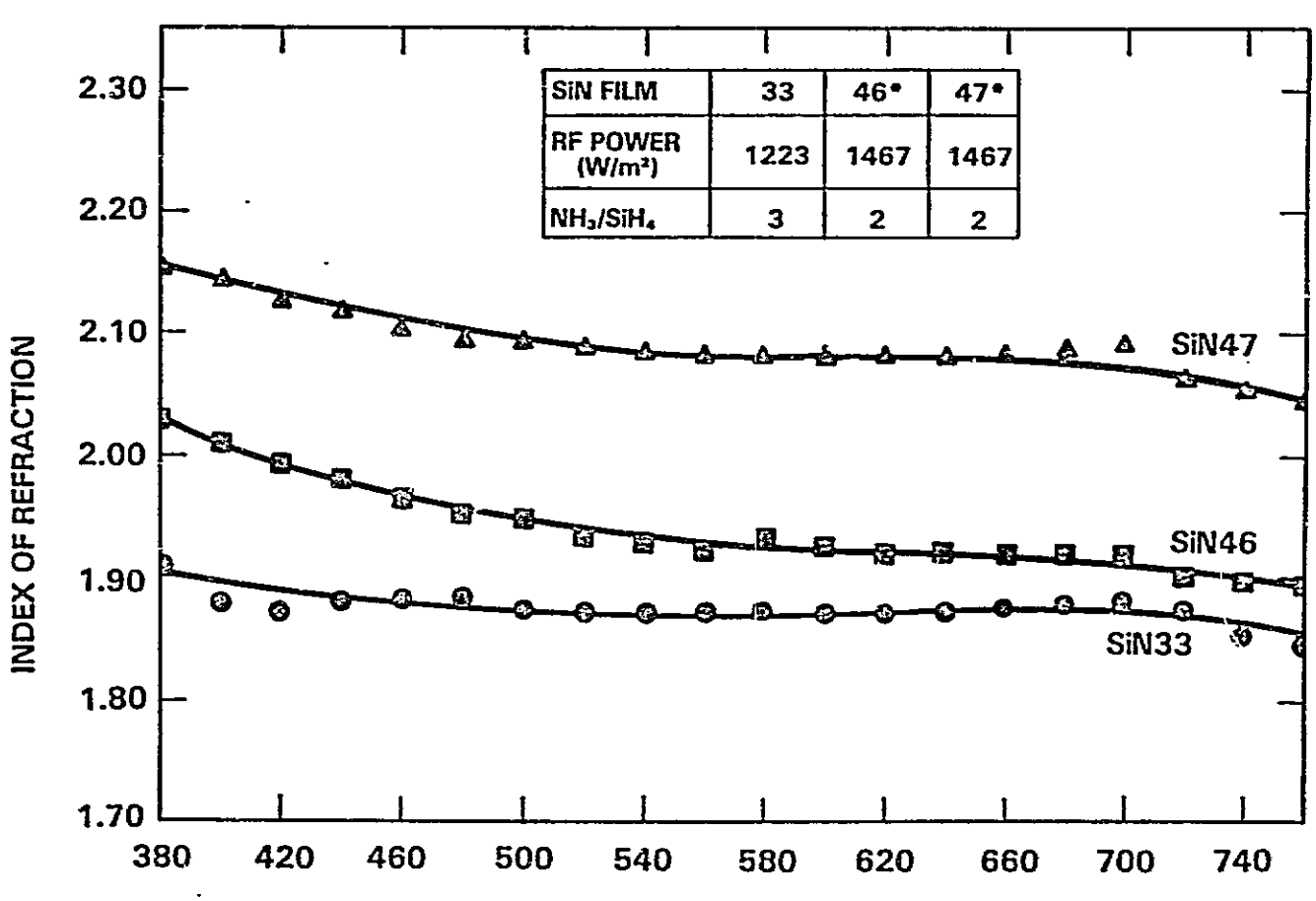

* CHAMBER WAS EVACUATED MORE CAREFULLY FOR SiN47 RELATIVE TO SiN46

Figure 6

Early in this program consideration was given to the use of SiN_x films for both layers in a double layer AR structure. By varying deposition parameters, one could deposit a high index film, and a low index film. Results for film SiN 119 indicate, however, that the high index films are too absorptive.

TABLE 2

CALCULATED VALUES OF ACTIVE AREA PHOTOCURRENT*

SiN_x FILM	OPTIMUM THICKNESS (Å)	ACTIVE AREA PHOTOCURRENT (mA/cm^2)
SiN-119	636	32.7
SiN-151	745	34.7
SiN_x with N = 1.9, K = 0	784	37.8

*Assumptions: (1) Phoenix, Az AM1 Spectrum
(2) Internal Photoresponse of Cell SiNP2 (See Section 5).

SILICON NITRIDE AS AN ANTI-REFLECTION COATING

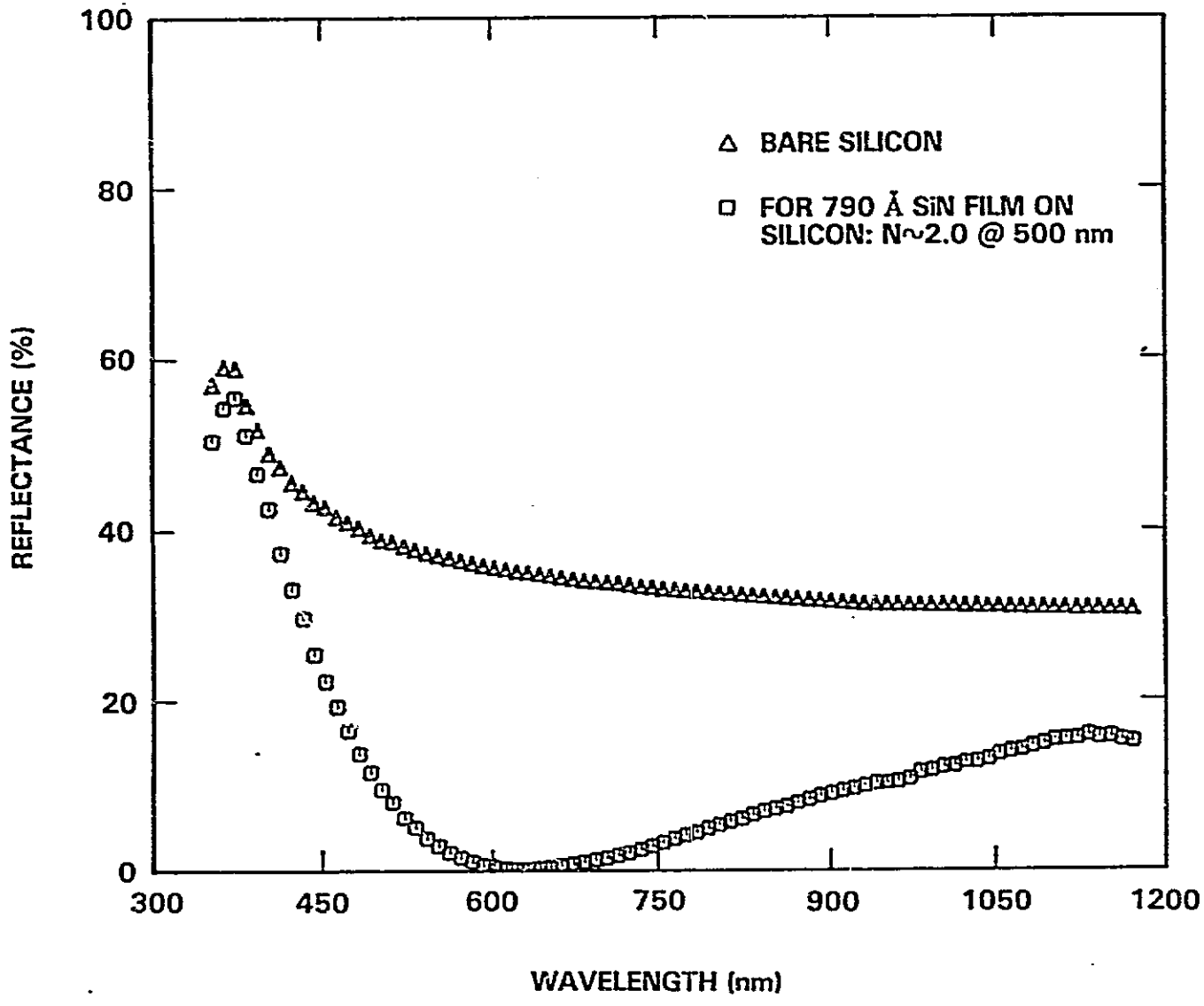

Figure 7

4. CHARACTERIZATION OF THE SiN_x/Si INTERFACE

A key objective of this program is to determine the passivation properties of PECVD SiN_x. Thus, measurements of interface state density at SiN_x/Si interfaces provide important information. The most relevant information is knowledge of the states at the SiN_x/Si(N^+) interface on a N^+/P cell. Investigations to date have involved high frequency C-V measurements on MIS structures based on moderately doped p-type substrates. In this section, the approach used for determining interface state density is briefly discussed, and then results are given studies relating deposition parameters and interface state densities for SiN_x/Si structures.

4.1 High Frequency C-V Measurement of Interface State Density

The density of states at the SiN_x/Si interface is presently determined by high frequency capacitance versus voltage (C-V) analysis. For the purposes of this analysis, a metal layer of approximately .004 cm^2 area is deposited onto the insulating layer. This metal layer is referred to as the gate. In addition, an ohmic contact is formed on the silicon base. This device, of course, is a MIS capacitor as shown in Figure 8.* The measurement consists of applying a series of voltages across the gate and the ohmic contact, nominally between +5 Volts and -25 Volts, and recording the high frequency capacitance and the applied voltage.

The necessary data is obtained using a PAR-410 capacitance meter in conjunction with an Apple II computer controlled digital-to-analog and analog-to-digital converters. A data acquisition program is in use which allows specification of the voltages at which the C-V data is to be read.

---

*It should be noted the "I" in MIS refers to an insulating layer which is typically 500 to 1000 A thick.

DENSITY OF STATES MEASUREMENT

VOLTAGE DISTRIBUTION

$$V = \Psi_S - \phi_{SM} - \frac{[Q_{POS} + Q_{SC}(\Psi_S)]}{C_o}$$

WHERE:

$$C_o = \frac{\varepsilon_{INS}}{d_{INS}} \qquad Q_{POS} = Q_{FC} + Q_{SS}$$

HIGH FREQUENCY CAPACITANCE

$$dV = dV_{INS} + d\Psi_S$$
$$= \frac{dQ_{SC}}{C_o} + \frac{dQ_{SC}}{C_D}$$
$$= \frac{dQ_{SC}}{C}$$

$$C^{-1} = C_o^{-1} + C_D^{-1}$$

$$C_D = C_D(\Psi_S)$$

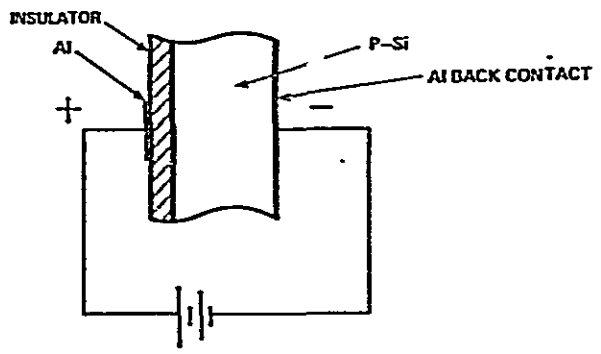

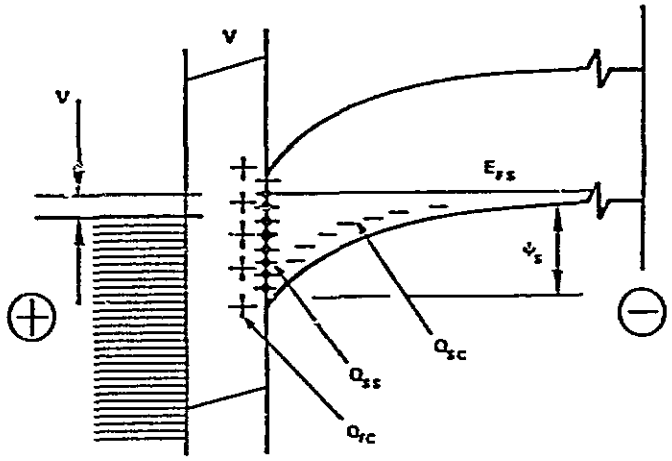

DATA ANALYSIS

- DETERMINE C_o FROM C VS. V AT $V < 0$.
- CHOOSE Ψ_S AND CALCULATE V.
- CALCULATE C VS. V FOR $Q_{POS} = 0$
- DETERMINE $Q_{POS} = Q_{INS} + Q_{SS}$ AS FUNCTION OF Ψ_S BY COMPARING EXPERIMENTAL RESULTS FOR C VS. V TO THEORETICAL RESULTS FOR C VS. V WITH $Q_{POS} = 0$.

$$Q_{POS} = C_O \times \Delta V$$

- D_{SS} GIVEN BY

$$D_{SS} = \frac{dQ_{SS}}{d\Psi_S} = \frac{dQ_{POS}}{d\Psi_S}$$

Figure 8

A machine language subprogram executes the actual control of the digital-to-analog converter and the reading of the C and V data through t' analog-to-digital converter. This allows acquisition of data at rates up to one point per millisecond, or slower if so specified. The main program is written in BASIC, and allows plotting of the data and results of data analyses.

When a voltage is applied to an MIS capacitor, a charge is induced in the semiconductor and at the interface by the electric field, as is shown in Figure 8. The magnitude of this charge is deduced knowing the applied voltage and the capacitance of the insulating layer. This charge is the sum of the space charge in the semiconductor, Q_{SC}, the interface state charge, Q_{SS}, and the fixed charge in the insulator, Q_{FC}. The space charge component can be evaluated by way of the capacitance measurement. From the capacitance, the width of the space charge layer in the semiconductor is deduced knowing the dopant concentration and the surface potential (Ψ_S). Q_{SC} can then be calculated and subtracted from the total charge to give the sum of Q_{FC} and Q_{SS}. Since the surface potential Ψ_S is also known at each voltage, the interface state density (D_{SS}), can be determined by differentiating this sum with respect to Ψ_S.

This method is accurate for interface state densities down to approximately $1x10^{11}$ states/cm^2/eV, but becomes inaccurate below this value. Present SiN_x/Si interfaces on moderately doped p-type silicon have in fact been characterized by surface state densities below this value. Thus, the problem of inaccuracy for low values of D_{SS} has become apparent. A more accurate method for analysis using the same MIS structures is presently nearing readiness for implementation at JCGS. In particular, the slow ramp capacitance versus voltage analysis will be utilized in the near future. Previous experience with this measurement at JCGS on nitride MIS devices has indicated injection of charge into the nitride during the slow voltage sweep. Such an occurence would invalidate the usual analysis procedure for slow ramp C-V data. To allow determination of the degree of charge injection during the significant part of the voltage sweep, the usual slow ramp

measurement has been augmented by the simultaneous measurement of the high frequency capacitance. Theoretical analysis indicates that such data will allow more detailed conclusions to be drawn concerning the charge distribution in the insulating layer.

4.2 Effects of Processing On The Interface State Density

There are several ways in which the SiN_x/Si interface can be affected. As a result, a study was conducted involving a matrix of processing approaches. Silicon substrates with resistivities of 2 Ω-cm and (100) orientation were used to fabricate MIS structures using SiN_x films on the order of 700 to 900 A thick for the insulating layer. Interface densities at mid-gap were determined from high frequency C-V measurements.

A processing sequence was defined by selecting one of two cleaning procedures, one of two surface oxide conditions, either nitrided or not nitrided, one of four procedures for growth of SiN_x films, and without any annealing or heat treatment at 350°C or 450°C. The two cleaning procedures were used, the RCA cleaning process and a more abbreviated process which does not include a peroxide step. The two surface oxide conditions were defined by a native oxide, and a thin, tunnelable oxide (≈20 A) formed by heat treating a wafer at 500°C for 30 minutes in oxygen. The nitrided process involves exposing a surface to a RF plasma using 16 W of power, NH_3 flowing at 70 sccm and with the platen at 270°C. After surface preparation (cleaning, oxide, nitrided or not), films were deposited with the RF power being 13 W or 75 W, and with the platen temperature at 150°C or 270°C. After a SiN_x film was grown, an aluminum gate was deposited and the surface state density determined using high frequency C-V measurements. The resulting mid-gap density is denoted "as deposited." The aluminum gates were then removed, and samples heat treated at 350°C or 450°C. After redepositing AL gates, mid-gap densities were measured again.

Figure 9 gives examples of results obtained in these studies. The high frequency capacitance is plotted versus gate voltage in Figure 9A. The density of states (D_{SS}) at the interface and net positive charge (Q_{pos}) in the nitride film are plotted versus surface potential (Ψ_S) in

(A)

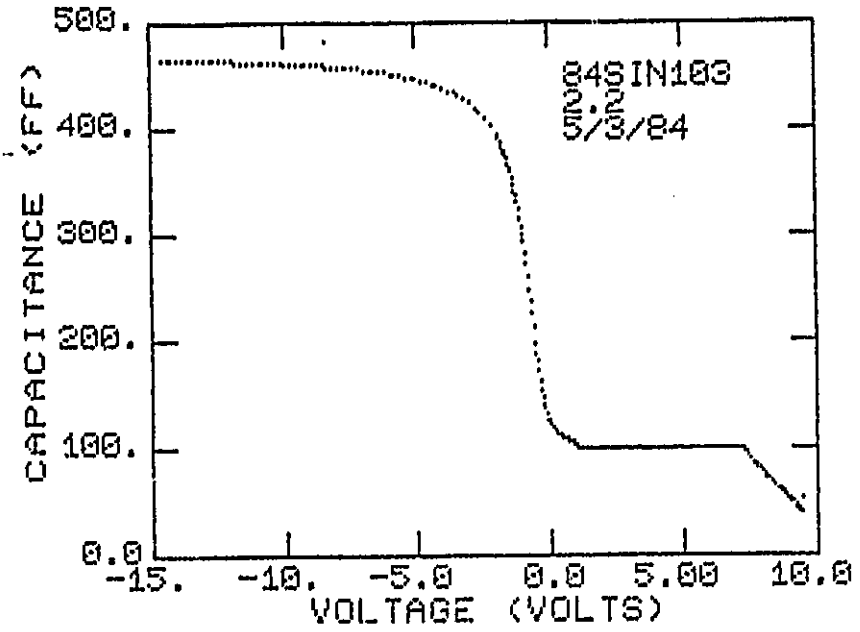

(B)

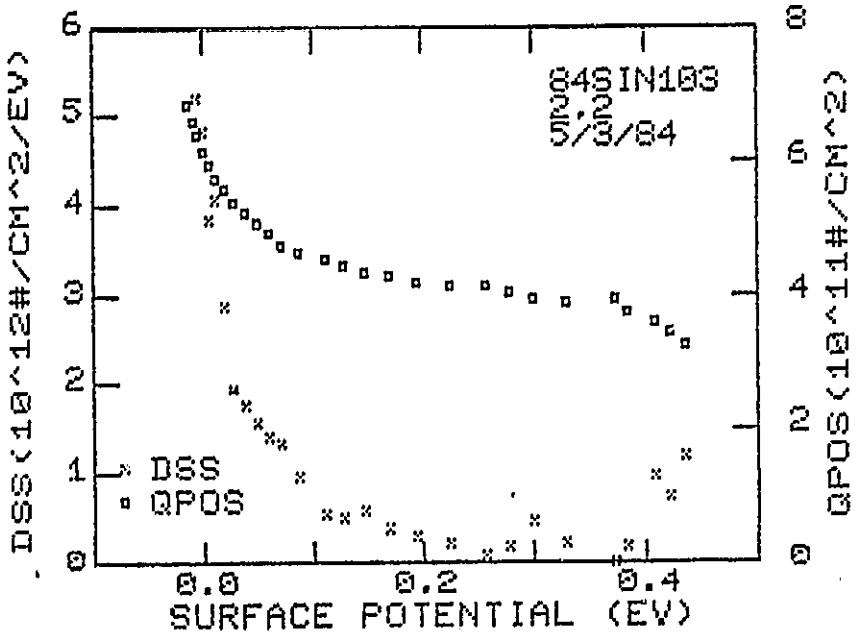

Figure 9. (A) High Frequency C-V Data.
(B) Calculated D_{ss} and Q_{pos} vs ψ_s.

Figure 9B. The mid-gap density is given by D_{ss} at $\Psi_s \approx 0.35V$. The actual mid-gap value of D_{ss} for this sample was 1.3×10^{11} $cm^{-2}eV^{-1}$. The interface processing involved an RCA clean, growth of a 20A oxide, nitriding the surface, and growth of SiN_x using 10 sccm SiH_4, 10 sccm NH_3 and 30 sccm Argon, RF power of 75 W and a platen temperature of 270^0C.

Figure 10 summarizes the results of the matrix study. Each rectangular entry in the figure shows results for the mid-gap values of D_{ss} on a logarithm scale from 10^{10} to 10^{13} $cm^{-2}eV^{-1}$. Each rectangular region gives results for MIS structures prepared with a particular surface preparation, SiN_x film growth conditions, and as grown or heat treated at 350^0C or 450^0C. The entries denoted by broken lines refer to $D_{ss} < 5 \times 10^{10}$ $cm^{-2}eV$, the detection limit of our present measurement technique.

Several key conclusions can be made from this study.

(1) SiN_x film deposition at low power (10 to 20 W) leads to lower surface state densities.

(2) Deposition at 270^0C is preferable for low surface state densities.

(3) Nitriding the silicon surface prior to SiN_x deposition results in low interface state densities.

The effect of nitriding is very significant.

Figure 11 illustrates the effects of heat treatment in more detail. The as deposited value of D_{ss} for the film grown at 150^0C is nearly 2×10^{12} $cm^{-2}eV^{-1}$. Heat treatment at 250^0C results in a reduced value of D_{ss}, namely, 6×10^{10} $cm^{-2}sec^{-1}$. Heat treatment at higher temperatures results in larger values of D_{ss}. It is generally thought that the reduction in D_{ss} is due to hydrogen diffusing to the interface where "dangling bonds" are "tied up." Further heat treatment causes a loss of hydrogen and increased D_{ss}. The values of D_{ss} for the sample grown at 270^0C are all below the detection limit. It is expected that the results are similar to those reported by Hezel and coworkers.[2] For a similar film, they obtained a minimum value for D_{ss} on the order of 6×10^9 $cm^{-2}eV^{-1}$. We are currently developing a capability for carrying out quasi-static C-V measurements. This approach should allow detection of D_{ss} values below 10^{10} $cm^{-2}eV^{-1}$.

RESULTS OF INTERFACE STATE STUDY OF SiN_x ON P-TYPE SILICON

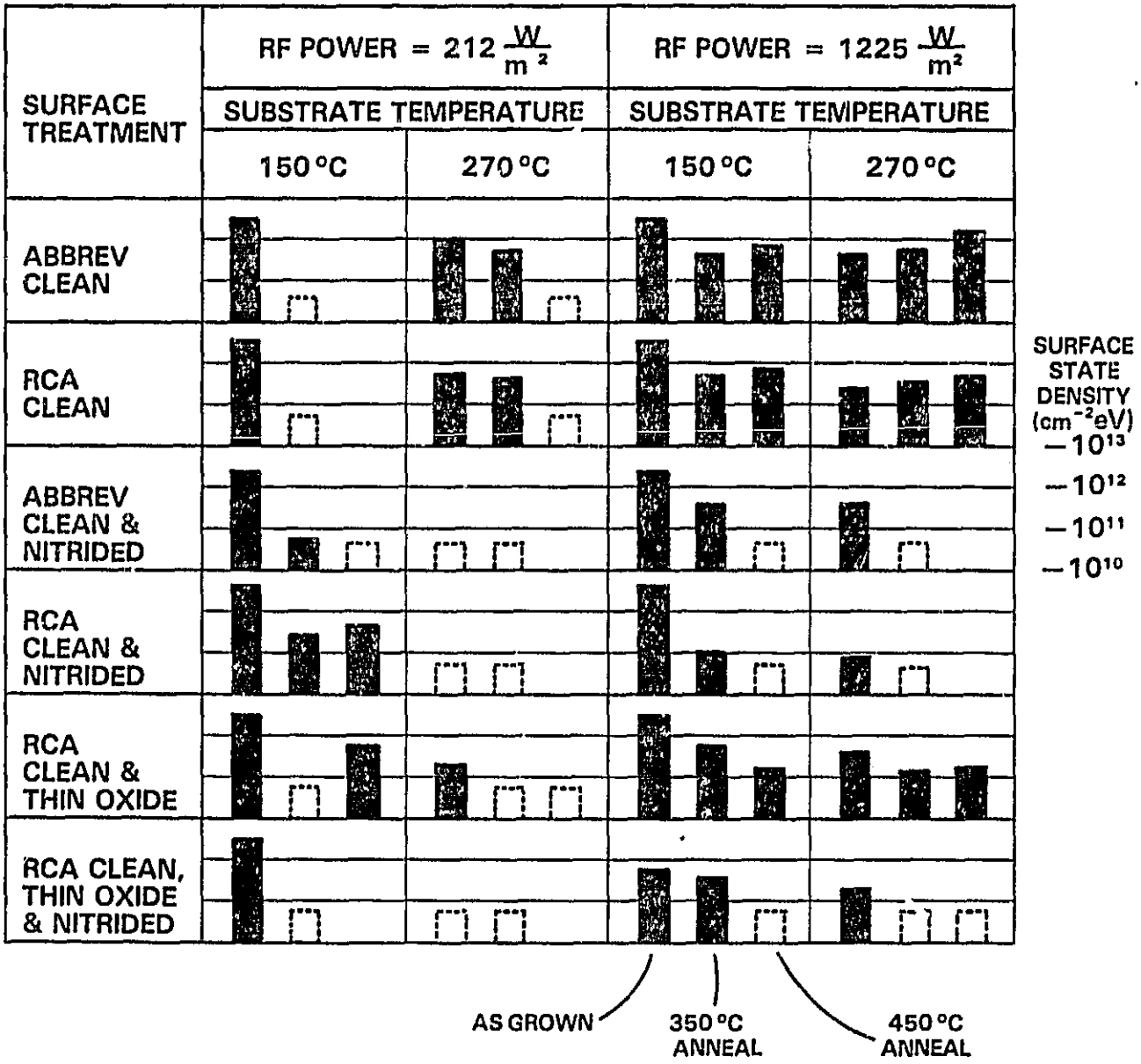

Figure 10

INTERFACE STATE DENSITY VS. ANNEALING TEMPERATURE FOR SiN_x ON P-TYPE SILICON

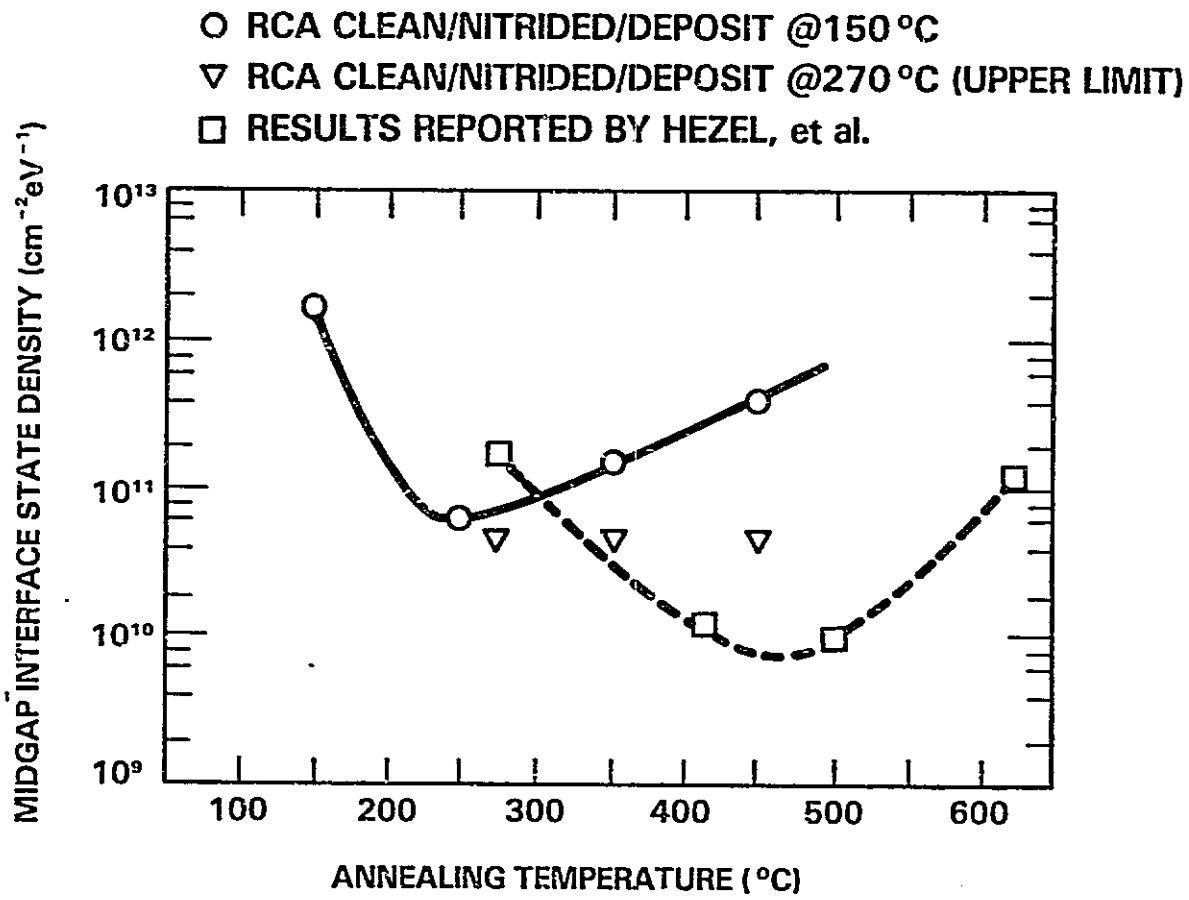

Figure 11

It should be emphasized that the results for interface state densities obtained in this matrix study were obtained for MIS structures based on SiN_x films, 700 A to 900 A thick, deposited onto 2 Ohm-cm, p-type FZ silicon substrates. The ohmic back contacts and metal gates were aluminum.

4.3 Surface Recombination Velocity

A key question concerns expected values of surface recombination velocity (S) for an interface between a SiN_x film and an N^+ surface of a p-type silicon substrate which has a diffused N^+/P junction at the front surface. S is approximately given by

$$S \simeq \sigma v_{th} D_{ss}(kT)$$

assuming $\sigma \simeq 10^{-14}$ cm^2 and $v_{th} = 10^7$ cm/sec for $D_{ss} \simeq 10^{12}$ cm^{-2} eV^{-1}. Even allowing σ to be larger, it seems clear that D_{ss} values on the order of 5×10^{10} $cm^{-2}eV^{-1}$ should give S-values $< 10^3$ cm/sec. The cells examined as part of this program do not exhibit such low values for S. Thus, it appears that the N^+ surface of N^+/P junctions must have larger values of D_{ss}. Nevertheless, it seems reasonable to expect that D_{ss} values obtained for MIS structures on moderately doped single crystal substrates provide guidance regarding the degree to which the silicon surface is passivated at the SiN_x/Si interface.

5. SURFACE RECOMBINATION VELOCITY DEDUCED FROM PHOTORESPONSE

Knowledge of the internal photoresponse of a solar cell, allows one to estimate the surface recombination velocity that can be obtained. This section includes a brief discussion of the JCGS photoresponse measurement system, internal photoresponse results for a silicon MINP cell passivated with 100 A of thermally grown SiO_2, and silicon cells provided by JPL coated with SiN_x.

5.1 Photoresponse Measurement And Analysis

The JCGS photoresponse system is described by the schematic diagram in Figure 12. A tungsten-halogen light source is utilized in a Bausch & Lomb high intensity monochromator equipped with collimating lenses. The monochromatic light is filtered to remove harmonic frequencies, then chopped by a Laser Precision Corp. Model OTX 532 chopper to allow phase sensitive detection to be utilized. The chopper operates at 32 Hz.

A Melles-Griot Plate beamsplitter with coating 007 and an AR coating on the back is mounted with the dielectric oriented towards the monochromator. Light incident on the beamsplitter then reflects to the cell (or substrate), or transmits to a pyroelectric detector. The cell is mounted on a vacuum chuck stand which is equipped with electrical contacts. Reflectance is measured by a silicon photocell mounted in a shielded enclosure opposite the cell mounting chuck. This reflection detector is shuttered to prevent multiple reflections when photoresponse is being measured.

The signals from either the solar cell under test, or the reflectance detector are then ratioed to the pyroelectric reference detector signal by a Laser Precision RK-5200 Power Ratiometer. This ratio is then outputted to a microcomputer which records the data for analysis on a mainframe computer. Calibration constants were determined by comparisons using an EG & G calibrated standard cell type UV-444BQ for photoresponse and a polished silicon wafer for reflectance. The theoretical values used for the wafer were verified by exchanging two wafers with Oak Ridge National Lab for integrating sphere and normal reflectance measurements.

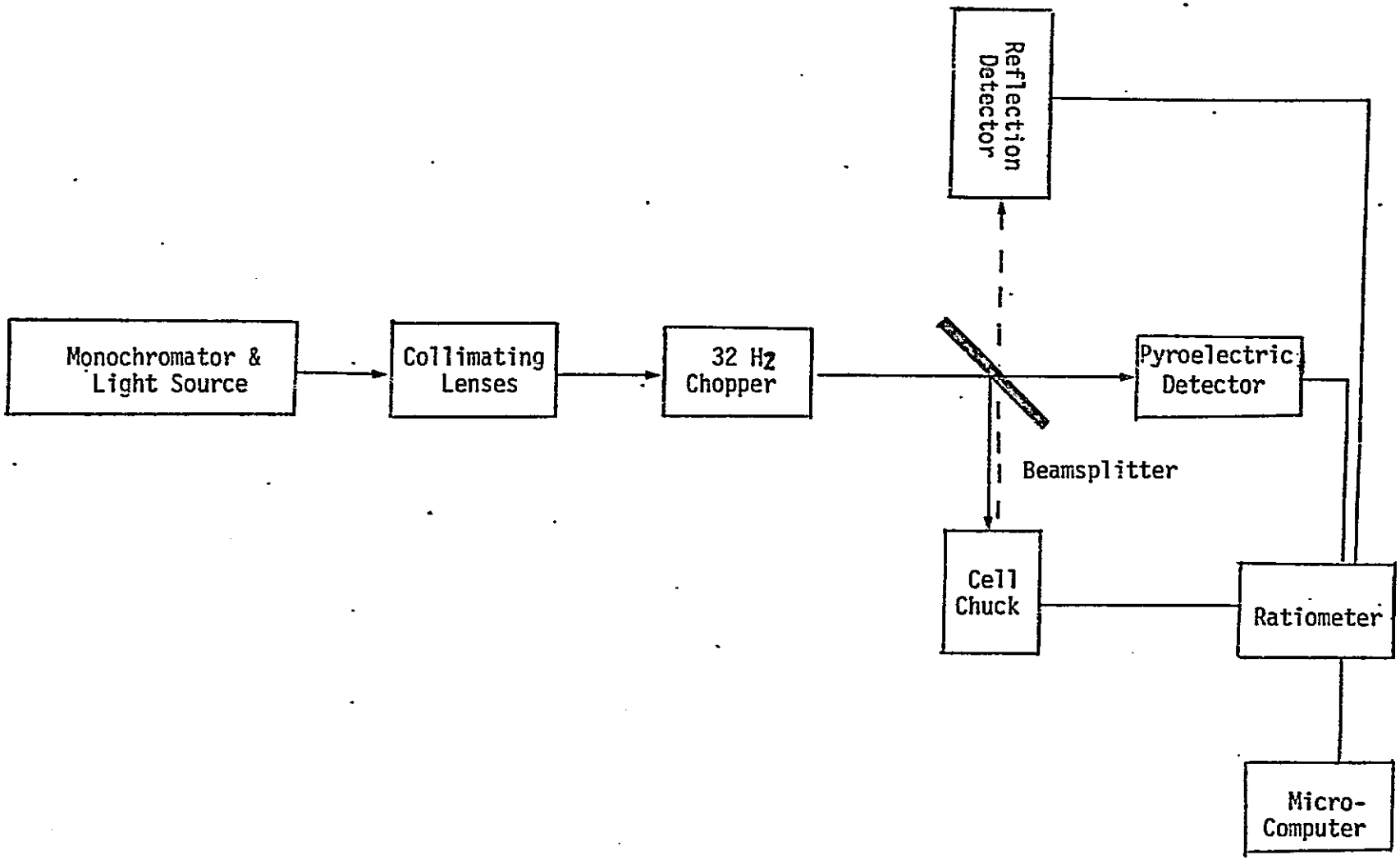

Figure 12. Schematic of Spectral Photoresponse System.

Data is taken from 350 to 1200 nm in 10 nm increments. By using a chopped beam, cells can be tested with or without an AM1 bias. Accuracy for normal reflection is within 1.5% and reproducibility for photoresponse is within 3%.

Figure 13 indicates the basic approach to photoresponse analysis. The photocurrent J_{PH} is measured for a given wavelength. The internal photoresponse S_{INT} is determined by

$$S_{INT} = J_{PH}/(T_\lambda \cdot N_\lambda \cdot q)$$

where N_λ refers to the incident photon flux and T_λ is the photon transmittance into silicon. The reflectance $R\lambda$ is measured. Thus, an upper limit to S_{int} is obtained from

$$S_{INT} \leq \frac{J_{PH}}{qN_\lambda (1-R_\lambda)}$$

If the optical constants and thickness of each AR layer are known, T_λ can be calculated. If the silicon cell has no AR coating, then one can obtain fairly accurate results by calculating reflectance from known optical constants for silicon. One of the best approaches for photoresponse analysis involves the use of an area on a cell where no grid lines exist and the transmittance into silicon can be accurately calculated.

5.2 Results For Silicon MINP Cell Passivated By 100 Å of SiO_2

Results for a silicon MINP cell made by JCGS are presented here to establish baseline properties to which cells coated with SiN_x can be compared. Figure 14 gives results for internal photoresponse of this cell. The front surface recombination appears to be in the range of 10^3 to 10^4 cm/sec. Fabrication details and cell structure are described in Table 3. Grid lines were excluded from a region slightly larger than the monochromator

INTERNAL PHOTORESPONSE ANALYSIS

THEORY

$$J_{PH}(\lambda) = S_{INT}(\lambda) \cdot T_\lambda \cdot N_\lambda \cdot q$$

$$S_{INT}(\lambda) = (S_{INT})_{EMITTER} + (S)_{\substack{DEPL. \\ WIDTH}} + (S_{INT})_{BASE}$$

$$T_\lambda = T_\lambda(N_{AR}, K_{AR}, N_{Si}, K_{Si})$$

$$= 1 - R_\lambda - A_\lambda$$

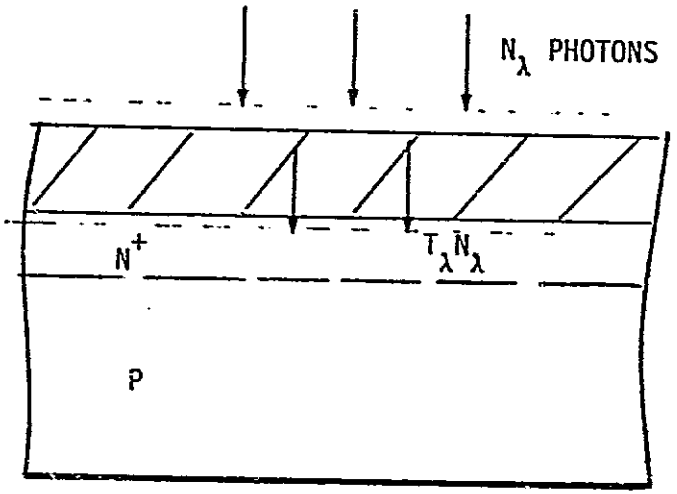

EXPERIMENT

MEASURE: $J_{PH}(\lambda)$, R_λ, N_λ and K_λ of SiN_x

ANALYSIS: HAVE OBTAINED $S_{INT}(\lambda)$ FOR CELLS WITH SIN_x LAYERS.
DETERMINED S_F ASSUMING A HOMOGENEOUS EMITTER.

Figure 13. Approach to Determine Internal Photoresponse.

INTERNAL PHOTORESPONSE VS. WAVELENGTH FOR SILICON N/P CELL WITH 100 Å SiO_2

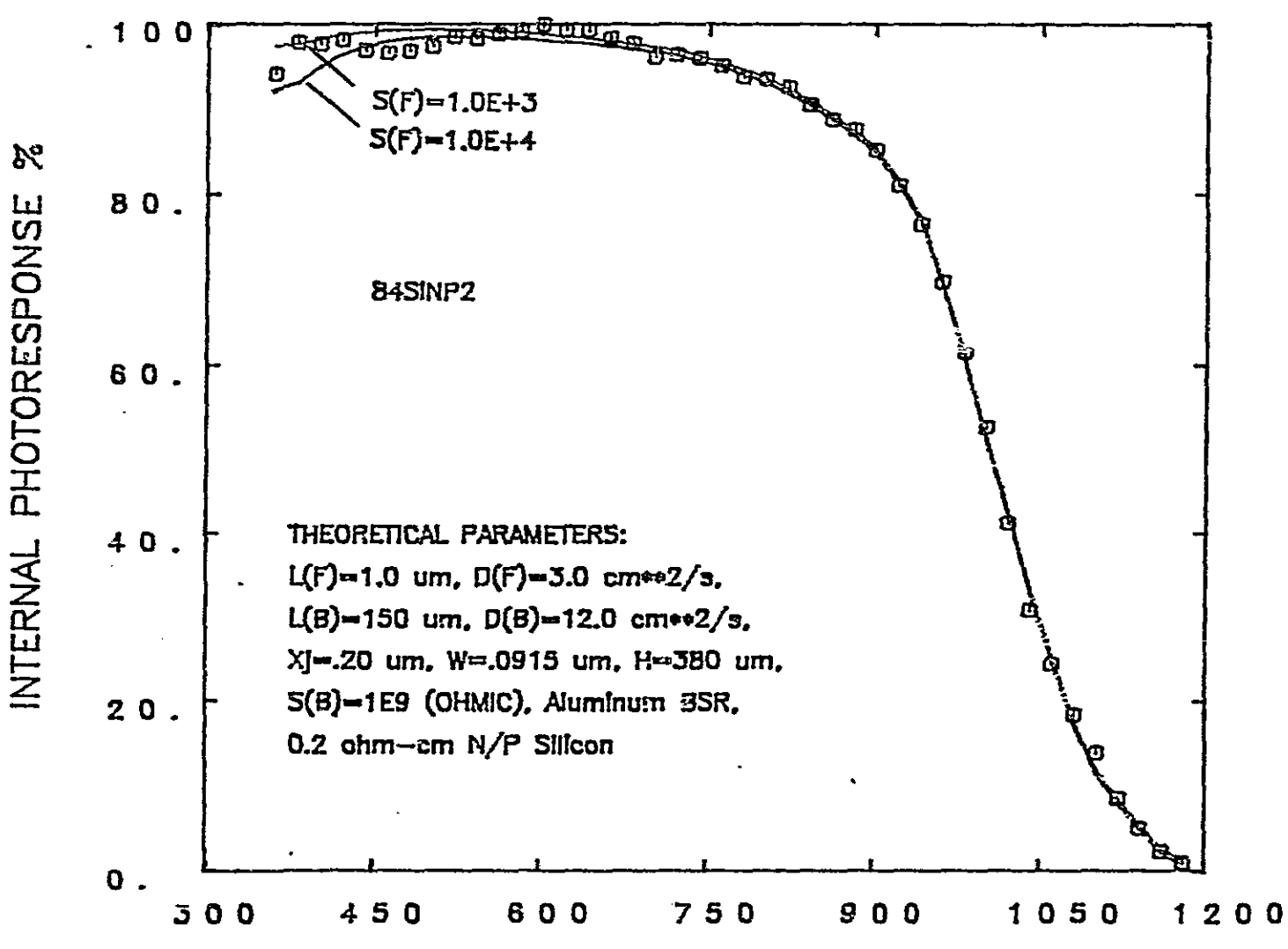

Figure 14

TABLE 3

PROPERTIES OF SILICON MINP CELL 84SiNP2

SILICON MATERIAL	P-TYPE FZ
BASE RESITIVITY	0.2 Ω-cm
JUNCTION DEPTH	0.15 to 0.25 μm
CELL THICKNESS	380 μm
BACK CONTACT	Aluminum
FRONT SURFACE PASSIVATION	100 A THERMAL SiO_2
MIS COLLECTOR GRID	Mg

beam size, namely, 4 mm x 7 mm. Since the only surface layer on the cell is approximately 100 A of SiO_2, there should be negligible absorption of the photon bean. As a result, the transmittance is accurately given by

$$T_\lambda = 1-R_\lambda$$

where R_λ is measured.

5.3 Results For JPL Terrestrial Standard Cells

JPL provided twelve cells referred to as "terrestrial standard" cells. These cells had collector grids but no AR coatings. Structural details are given in Table 4. Six of these cells were made on material with (100) orientation and six with (111) orientation. Cells were characterized in detail. In particular, absolute spectral photoresponse was measured for each cell before and after SiN_x film growth. Dark and illuminated current-voltage characteristics were also acquired for the cells before and after SiN_x deposition. In addition, I-V analyses for a range of temperatures were conducted for six of these cells. The I-V results are discussed in Section 6.

SiN_x was deposited on these cells using a procedure suggested by the results of the "passivation matrix" study. Cells surfaces were nitrided and then SiN_x films were grown with the platen at 270°C and with the RF power level at 13 W.

TABLE 4

STRUCTURE OF JPL TERRESTRIAL STANDARD CELLS

SILICON MATERIAL	CZ
BASE RESISTIVITY	2 Ohm-cm
JUNCTION	N^+/P
JUNCTION DEPTH	≈ 0.4 μm
CELL THICKNESS	
BACK CONTACT	Aluminum
FRONT CONTACT	Ti/Ag
AR COATING	None

Typical results are shown in Figure 15. Results are shown for internal photoresponse determined for cell JPL2 before and after SiN_x deposition. Calculated values of $S_{INT}(\lambda)$ are shown as solid lines for the front surface recombination velocity (S_F) being 10^4, $3x10^4$ and 10^5 cm/sec. The bare cell was characterized by $S_F \approx 3x10^4$ cm/sec. After SiN_x deposition, S_F decreased slightly to $S_F \approx 2x10^4$ cm/sec. Thus, some passivation appears to have been achieved. S_{INT} was determined by calculating T_λ assuming N and K values of the SiN_x film to similar to those for film 84-151 shown in Figure 3.

5.4 Results For Shallow Junction JPL Cells

Another group of cells was supplied by JPL which have more shallow junctions than the terrestrial ,tandard devices. The structure of these cells is summarized by Table 5. Both N^+/P and P^+/N cells were provided. The base resistivity of these cells is also in the range of 1 to 3 Ohm-cm. Junctions are on the order of 0.2 μm. Finally some cells had $Si0_x$ AR coatings already applied.

TABLE 5

STRUCTURE OF SHALLOW JUNCTION JPL CELLS

MATERIAL	(111) FZ P-Type (N^+/P) (100) CZ P-Type (N^+/P) (100) CZ N-Type (P^+/N)
BASE RESISTIVITY	1-3 Ohm-cm
JUNCTION	N^+/P and P^+/N
JUNCTION DEPTH	0.15 to 0.2 μm for N^+/P >0.2 μm for P^+/N
CELL THICKNESS	320 μm
AR COATING	Some cells bare and some with $Si0_x$ AR

INTERNAL PHOTORESPONSE VS. WAVELENGTH FOR JPL CELL

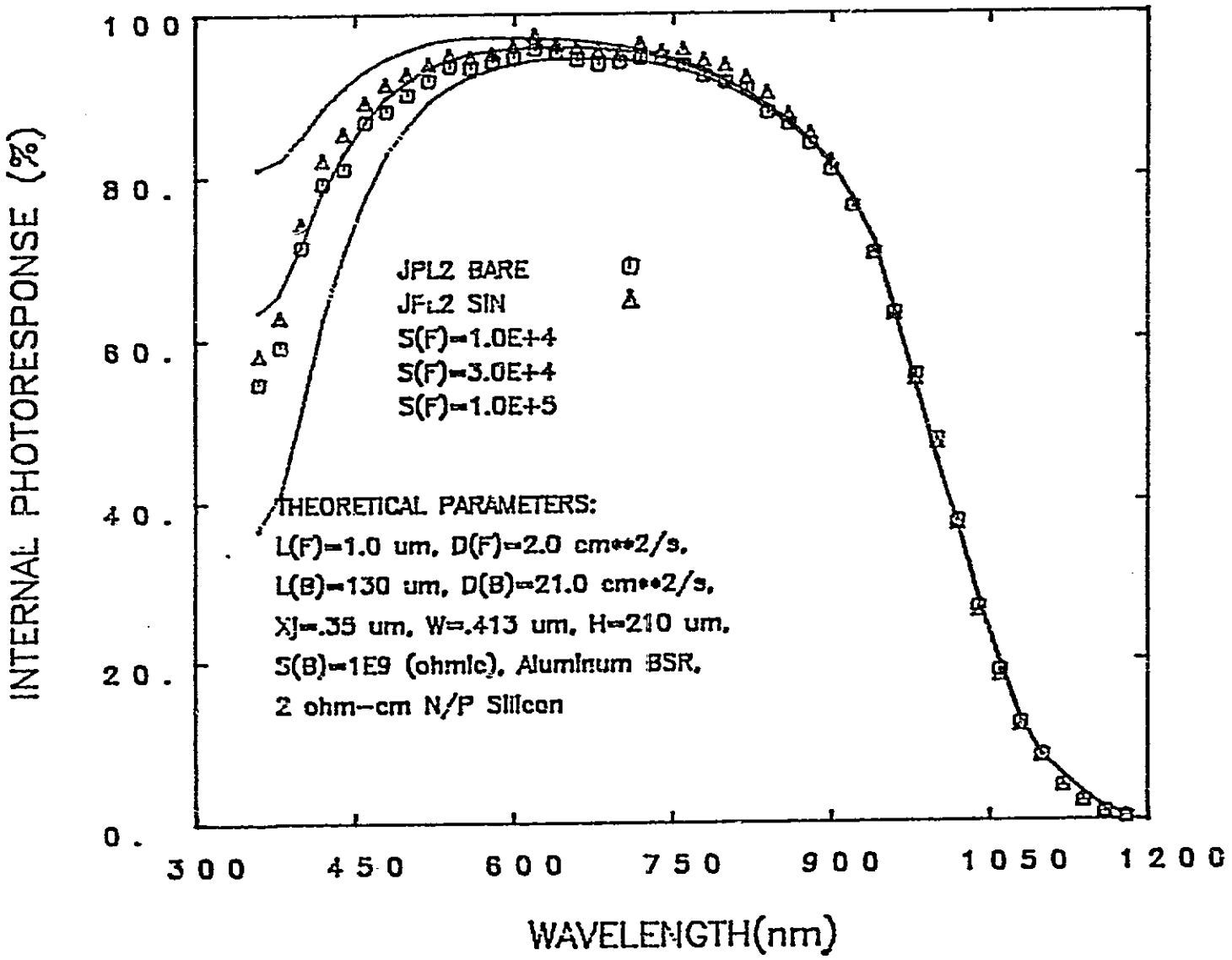

Figure 15

Typical results for cells coated with SiN_x are shown in Figure 16. The values of S_F were typically 10^5 cm/sec before and after SiN_x. These cells were coated during a time period when the PECVD system had a significant leak. Thus, it is reasonable to expect that SiN_x films grown on the second group of JPL cells are lower quality than those films grown on the first group. Witness p-type wafers were coated with SiN_x films during the SiN_x depositions for both JPL2 and JPL8-5. MIS structures fabricated with these witness wafers were characterized by C-V analysis, and found to have:

Witness JPL2 $D_{ss} \approx 5 \times 10^{10}$ $cm^{-2}eV^{-1}$
Witness JPL8-5 $D_{ss} = 7 \times 10^{11} cm^{-2}eV^{-1}$

Thus, although the interface state densities measured on moderately doped p-type material are probably lower than the interface state density on highly doped N^+ surface, the relative values are probably significant. The D_{ss}-values for the two witness wafers suggest that higher quality films were being deposited during the time period that the terrestrial standard cells were being coated with SiN_x. However, it should be noted that the second group of cells had front surface recombination values on the order of 10^5 cm/sec. Such a value indicates a relatively large surface state density. It is possible that the nature of the N^+ surface of a N^+/P device before AR deposition determines a lower limit for S_F.

INTERNAL PHOTORESPONSE VS. WAVELENGTH FOR JPL CELL

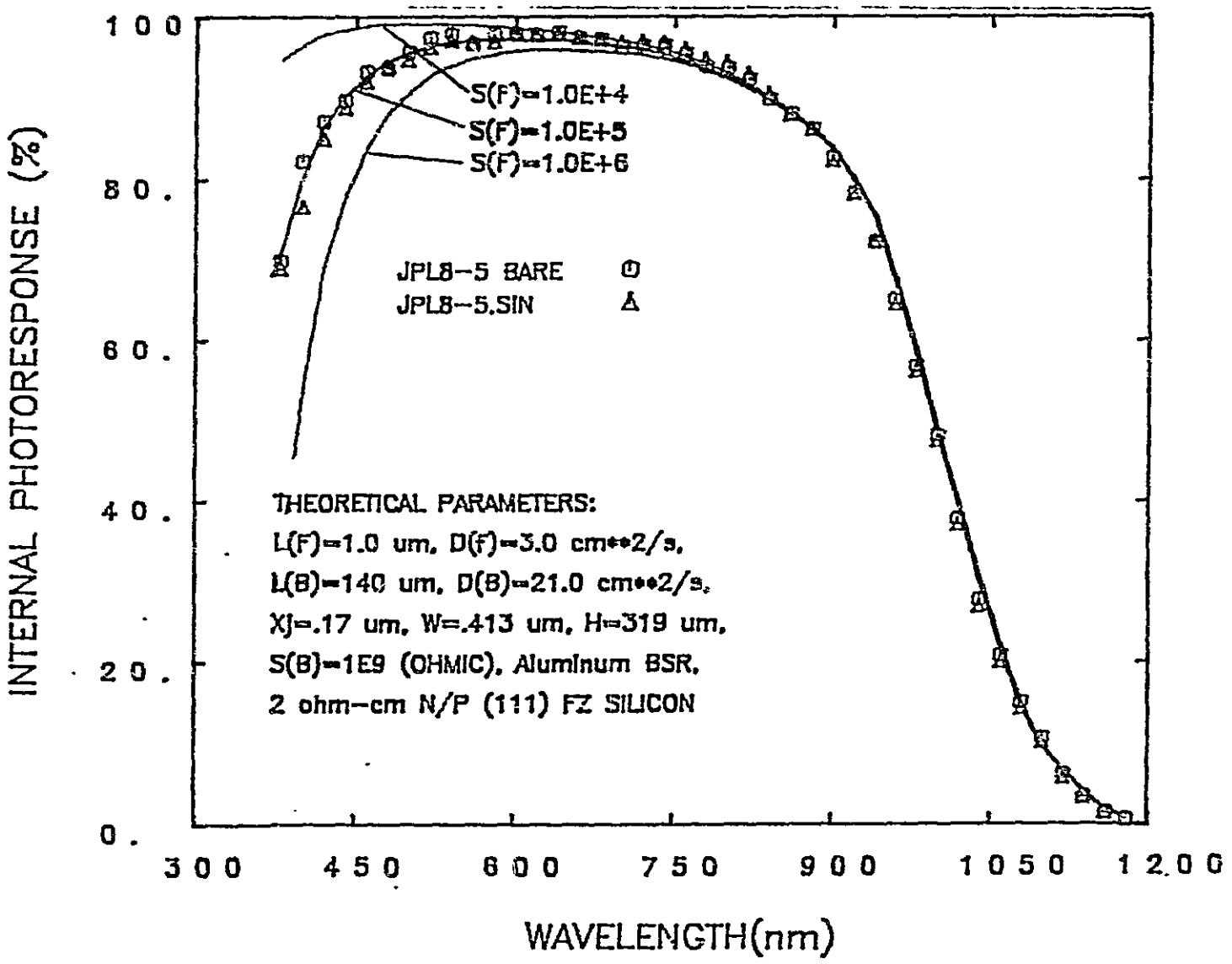

Figure 16

6. CURRENT-VOLTAGE ANALYSES OF SILICON N^+/P CELLS

Current-voltage analyses of the JPL cells were investigated in an effort to identify current loss mechanisms. The key objective of this work was to determine if the JPL cell performance was limited by emitter recombination. If a cell is limited by emitter recombination, then under some circumstances one can estimate the surface recombination velocity. Thus, I-V analyses have been conducted in conjunction with inernal photoresponse studies to provide additional information about surface recombination losses. In this section, a brief discussion concerning the theory of current-voltage characteristics is given, followed by discussions of results for a silicon MINP cell and the two groups of JPL cells.

6.1 Theory of Current-Voltage Characteristics

There are numerous possible current loss mechanisms which may dictate the I-V characteristics of silicon solar cells. Six possible mechanisms are described by Figure 17. In our experience with relatively high efficiency silicon solar cells all of these mechanisms can be important with the possible exception of field emission (#5), and losses due to shunt resistance. All of the other mechanisms can be significant in cells with AM1 efficiencies greater than 15%, say.

Silicon cell I-V characteristics usually can be interpreted in terms of two current mechanisms operating in parallel, a low voltage mechanism and a large voltage mechanism. We find that the low voltage mechanism usually can be interpreted as a tunneling mechanism as described by No. 4 in Figure 17. This loss mechanism seems to be associated with edge effects. One should not eliminate the possibility of tunneling via defects in the depletion region, especially for cells of very high efficiency. The low voltage mechanism can limit the fill factor, and thus must be reduced to some acceptable level.

THEORY FOR CURRENT-VOLTAGE CHARACTERISTICS

1. EMITTER RECOMBINATION CURRENT

$J = J_{OE}[\exp(\frac{V}{nkT}) - 1]$

$n = 1$

FOR RM TEMP ANALYSIS:

$J_{OE} = \frac{qn_i^2}{N_D(E_{fl})} \cdot GF$

GF IS A FCT OF W_H, S_P, D_{PO} & τ_P

FOR INTERPRETATION OF TEMPERATURE DEPENDENT DATA:

$J_{OE} = J_{OO}(T) \exp(\frac{-\phi}{kT})$

$\phi = 1.20 - (\Delta E)_{\substack{\text{EMITTER} \\ \text{BGN}}}$

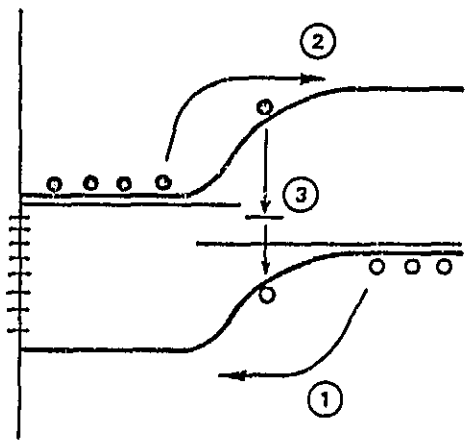

2. BASE REGION RECOMBINATION CURRENT

$J = J_{OB}[\exp(\frac{V}{nkT}) - 1]$

$n = 1$

$J_{OB} = \frac{qn_i^2}{N_A} \frac{L_D}{\tau_n} \cdot G_F$

$= J_{OO}(T) \exp(\frac{-\phi}{kT})$

$\phi = 1.20 - (\Delta E)_{\substack{\text{BASE} \\ \text{BGN}}}$

3. DEPLETION LAYER RECOMBINATION CURRENT

$J = J_{OR} \exp(\frac{V}{nkT})$ $V >> kT$

$J_{OR} = J_{OO} \exp(\frac{-\phi}{kT})$

$\phi = (E_t - E_v)$ OR $(E_c - E_t)$ $\quad n = 1$ TO 2

FOR $n \simeq 2$, $\phi \simeq E_g/2$ $\quad$ FOR $n \simeq 1$, $\phi \simeq 0.8$ eV

4. TUNNELING/RECOMBINATION

$J = J_{OT} \exp(BV)$ $\quad V >> kT$

B TEMPERATURE INDEPENDENT

$J_{OT} = J_{OO} \exp(\frac{-\phi}{kT})$

ϕ TYPICALLY 0 TO 0.5 eV

5. FIELD EMISSION

$J = J_{OF} \exp(CV)$

$C = \frac{1}{nkT} + B$

$J_{OF} = J_{OO} \exp(-\phi/kT)$

$\phi = fV_{bi}$ $\quad f = n^{-1}$

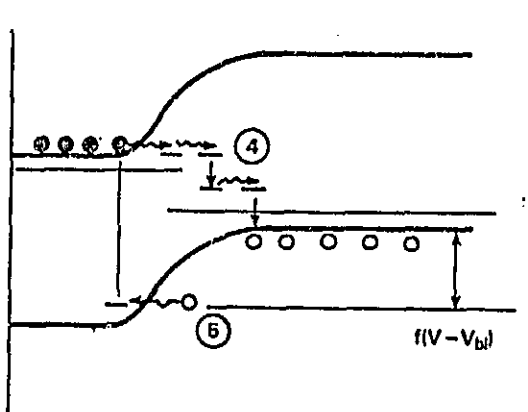

6. EDGE LEAKAGE CURRENTS

CURRENT MECHANISMS (3), (4) OR (5)

USUAL SHUNTING MECHANISM
$J_{SH} = V/R_{SH}$

Figure 17

The large voltage mechanism is determined by either mechanism 1, 2 or 3. This mechanism dictates the value of V_{OC} and FF for most relatively efficient silicon cells. The limiting performance of a N^+/P cell is determined of course, by base region recombination (#2). It is questionable whether a base limited cell has been achieved. Based on the information available, we contend that the 19% cell produced by Green and coworkers is not quite base limited.[3] One can certainly argue that none of the silicon cells reported to exhibit efficiencies in the 16% to 18% range are base limited.

Emitter recombination is usually identified as the limiting mechanism. We have analyzed I-V characteristics of JCGS MINP cells as well as efficient cells fabricated by Spire and ASEC (JPL cells). It seems clear that one cannot eliminate depletion layer recombination as the limiting mechanism for many cells. This mechanism is commonly identified with n=2. As clearly indicated in the original work by Sah, et al., the n-value can actually be close to one.[4] Thus, it is quite possible to have depletion layer recombination via a trap level 0.1 to 0.2eV from one of the band edges, resulting in $n \approx 1.0$ to 1.1 and ϕ of 0.8 to 0.9 eV. The key parameter which suggests such a mechanism is the activation energy. Whereas ϕ is in the range of 1.0 to 1.2 eV for emitter recombination, $\phi < 1.0$ eV for depletion region recombination. It should be noted that an impurity density of only 10^{14} cm^{-3} can lead to depletion region recombination with parametric values similar to those commonly determined in I-V analyses.

Emitter recombination is, of course, often the limiting current loss mechanism. The analytical treatment described in Figure 17 is an outline of the approach developed by Fossom and Shibib.[5]. This approach accounts for band gap narrowing, Fermi-Dirac statistics and Auger recombination. Calculated values of J_{oE} versus the surface dopant concentration (N_S) for a range of values for S are shown in Figure 18. The calculations are for a junction depth of 0.2 μm. J_o-values due to base region recombination for 15 mil cells utilizing 2 Ohm-cm and 0.2 Ohm-cm material are also shown. It should be emphasized that if emitter recombination current dominates, one should observe n=1 and $\phi \approx 1.0$ to 1.2 eV.

EMITTER J_o VS. SURFACE DONOR CONCENTRATION FOR SHALLOW JUNCTION N/P CELL

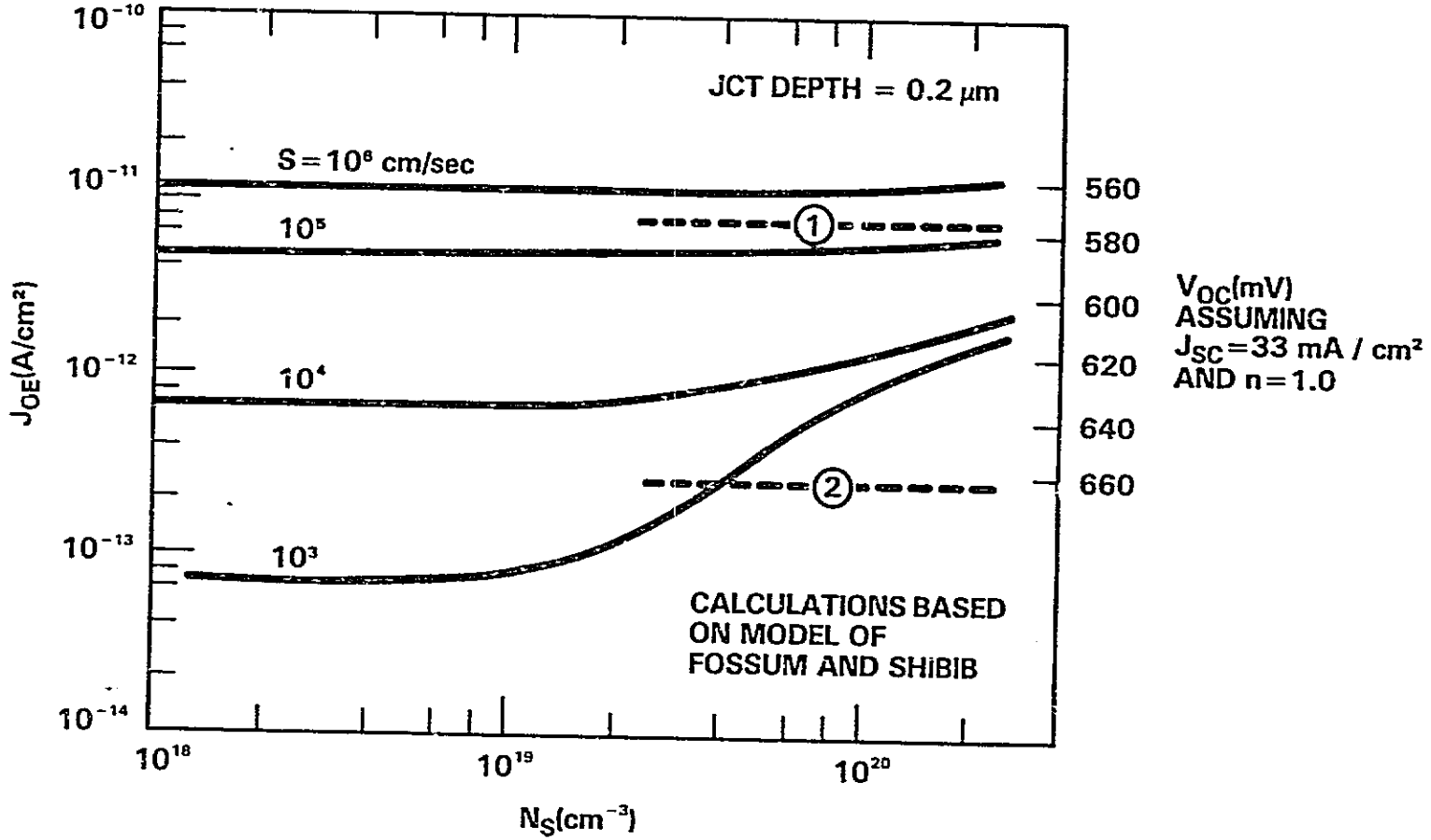

1 J_{OB} FOR 2 Ohm-cm N/P CELL WITH THICKNESS OF 15 MILS, L(BASE) = 130 μm, D = 21 cm^2sec^{-1} (APPROXIMATE CELLS PROVIDED BY JPL).

2 J_{OB} FOR 0.2 Ohm-cm N/P CELL WITH THICKNESS OF 15 MILS, L(BASE) = 150 μm, D = 21 cm^2sec^{-1}.

Figure 18

6.2 Approach to Current-Voltage Analyses

The approach to I-V analysis is summarized in Figure 19. Typically 30 to 100 data points are used to determine I_{01}, B, I_{02} and n. We find that I-V data can usually be fit with an average absolute error of less than 0.3%.

Current versus voltage data are taken using a microcomputer based data acquisition system. The Micro-computer is interfaced to a Datel-Intersil 16 bit digital-to-analog converter and a Data Translation 14 bit analog-to-digital converter. The A/D converter has a differential input amplifier stage having gains of 1, 10, 100 and 500. Current to voltage conversion is accomplished with the op-amp sub-circuit. Selection of the gains and of the sense resistors are controlled by the computer. Separate data acquisition programs are used to take the illuminated and dark I-V data, due to the different requirements of the two measurements. The dark I-V routine assumes unipolar current and voltage and selects the gain and sense resistor combination throughout the measurement for the sake of speed. Current versus voltage data are taken in a temperature controlled vacuum cryosat from 100°C to + 100°C. For the illuminated I-V data, cells are illuminated by a single ELH lamp through a window in the chamber. The lamp is set at an intensity to give approximately the same short circuit current measured under a calibrated ELH simulator.

Dark I-V results for one of the 0.2 μm junction JPL cells are shown in Figure 20. I-V data are shown for several temperatures. A $\text{Log}J_0$ vs T^{-1} plot is also shown. The J_0 referred to in the $\text{Log}J_0$ vs T^{-1} plot is the large voltage J_0. The break in this plot indicates that the nature of the large voltage mechanism changes over the temperature range considered. The activation energy associated with this mechanism is ≈ 1.0 eV for temperatures near ambient. The break in the $\text{Log}J_0$ vs T^{-1} plot is farily common, and needs to be understood.

APPROACH TO DARK I-V ANALYSIS

I-V RELATIONSHIP ($V_j >> kT$)

$$I_{MEAS} = I_j + V_j/nkT$$

$$V_j = V_{MEAS} - R_S I_{MEAS}$$

$$I_j = I_{o1} \exp(BV_j) + I_{o2} \exp(V_j/nkT)$$

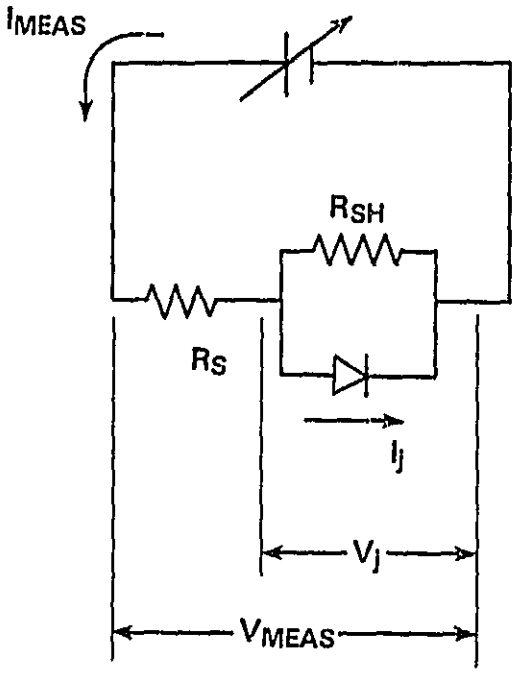

FITTING PROCEDURE

1. SELECT R_S AND R_{SH}
2. GENERATE (I_j, V_j)
3. CONSIDER (I_j, V_j) FOR REGION 1

   $I_j \simeq I_{o1} \exp(BV_j)$

   $\text{Log}_e(I_j) = \text{Log}_e(I_{o1}) + BV_j$

   LEAST SQUARES FIT $\Rightarrow I_{o1}$, B

4. CONSIDER (I_j, V_j) FOR REGION 2

   $I_{j2} = I_j - I_{o1} \exp(BV_j)$

   $= I_{o2} \exp(V_j/nkT)$

   LEAST SQUARES FIT $\Rightarrow I_{o2}$, B

5. ITERATE BETWEEN REGIONS 1 AND 2 UNTIL ACHIEVE CONVERGENCE.
6. CARRY OUT STEPS 1 THROUGH 5 FOR ARRAY OF R_S AND R_{SH} VALUES. SELECT VALUES OF PARAMETERS WHICH PROVIDE BEST FIT TO DATA.

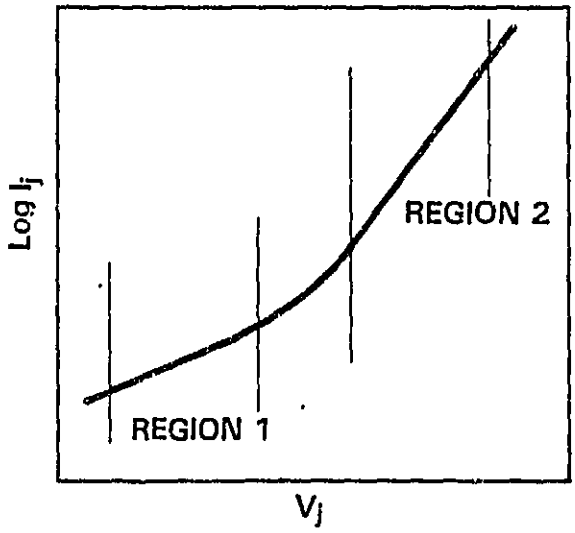

Figure 19

ANALYSIS OF TEMPERATURE DEPENDENT I-V CHARACTERISTICS FOR JPL CELL

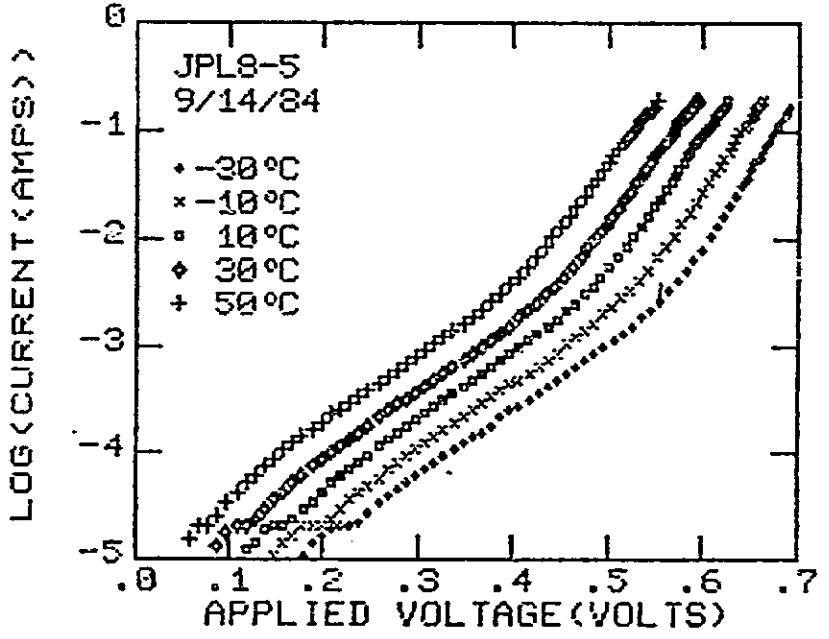

I-V DATA

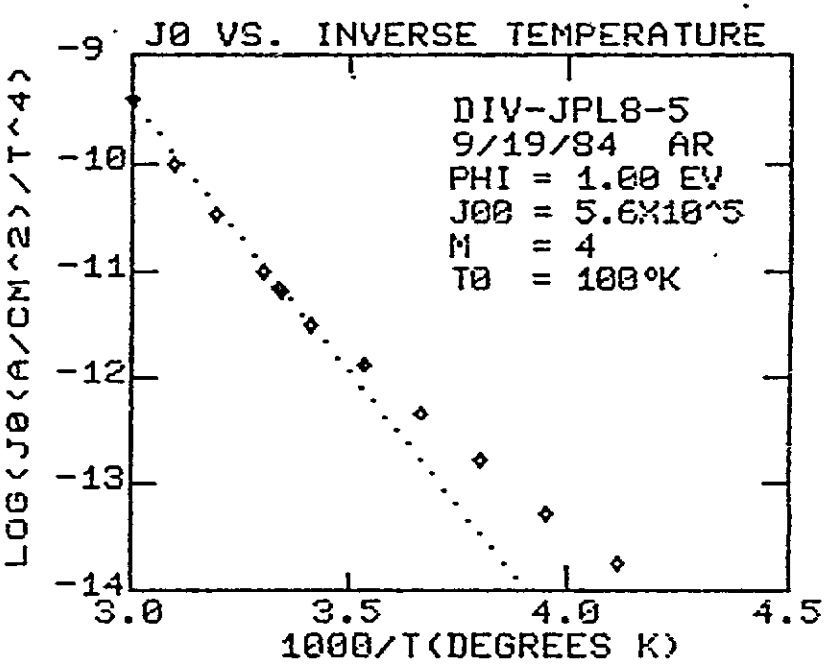

ACTIVATION ENERGY ANALYSIS

Figure 20

6.3 JPL Terrestrial Standard Cells

Current-voltage data were acquired over a range of temperatures for four cells before and after Si-N deposition. I-V parameters determined at 28°C are given in Table 6. Also shown in Table 6 are values for the activation energy ϕ , which is determined from results for I-V parameters obtained over a range of temperatures.

These cells exhibit two current mechanisms, a low voltage and a high voltage component. The low voltage component behaves as a tunneling mechanism. The high voltage mechanism is described in the usual manner, namely,

$$J_2 = J_{02} \exp (V/nkT).$$

The n-values are typically 1.10. It should be noted that parameters indicated in Table 6 allow one to fit the I-V data to within 0.2 to 0.3%.

Values for J_{02} are typically in the 10^{-11} to 10^{-10} A/cm^2 range, and n is usually near 1.10. Since n is significantly different than 1.0, it appears that the large voltage mechanism is due to depletion region recombination. The value of J_{02} is also too large for either emitter recombination or base region recombination.

Very little change was observed in the large voltage mechanism after SiN_x was deposited onto these cells. This result is consistent with the conclusion that depletion layer recombination is the dominant loss mechanism at large voltages. It appears that the diffusion process causes required for the 0.4 μm junction introduces too many trap levels in the depletion region.

6.4 Shallow Junction JPL Cells

Current-voltage analyses were also carried out for JPL cells with junction depths of 0.2 μm. Results for these cells are shown in Table 7. Also shown are I-V parameters for JPL-6, a deep junction cell, and a JCGS MINP cell 84-2. The 0.2 μm JPL cells show both emitter recombination and

TABLE 6

I-V PARAMETERS FOR JPL TERRESTRIAL STANDARD CELLS

CELL	ORIENTATION	EFF (%)	I_{SC} (mA)	V_{OC} (mV)	B (V^{-1})	J_{01} (A/cm^2)	n	J_{02} (A/cm^2)	ϕ (eV)	COMMENT
JPL-3 (3-6)	(100)	--	DARK	--	8.4	1.1 E-5	1.05	1.7 E-11	.97	BARE
		--	DARK	--	10.6	6.7 E-6	1.09	3.3 E-11	.67	SiN
		9.54	86.0	576	5.8	3.3 E-5	1.14	1.1 E-10	.95	BARE
		13.08	124.0	586	13.6	1.9 E-6	1.10	2.9 E-11	--	SiN
JPL-6 (2-6)	(100)	--	DARK	--	10.7	2.9 E-6	1.11	5.7 E-11	.72	BARE
		--	DARK	--	13.4	2.7 E-7	1.07	2.1 E-11	.96	SiN
		9.57	87.0	573					--	
		13.54	128.0	584					--	
JPL-13 (4-5)	(111)	--	DARK	--	8.3	1.7 E-5	1.10	3.4 E-11	.88	BARE
		--	DARK	--	9.9	7.4 E-6	1.11	4.1 E-11	.94	SiN
		9.72	88.0	580	3.2	1.6 E-4	1.24	4.9 E-10	.92	BARE
		14.00	126.0	592	1.1	5.5 E-4	1.40	2.5 E-9	--	SiN
JPL-16 (3-6)	(111)	--	DARK	--	9.1	6.8 E-6	1.07	1.9 E-11	1.05	BARE
		--	DARK	--	12.6	3.0 E-6	1.04	1.2 E-11	.80	SiN
		9.83	87.0	579	8.0	1.1 E-5	1.11	5.6 E-11	1.04	BARE
		13.09	125.0	590	11.2	6.2 E-6	1.15	7.3 E-11		SiN

NOTE: I-V Data Analysis Based On Assuming:

$$J = J_{01} \exp(BV) + J_0 \exp(V/nkT) \qquad V \gg kT$$

and $$J_0 = J_{00} \exp(\phi/kT)$$

TABLE 7

I-V PARAMETERS FOR DARK CHARACTERISTICS

CELL	JCT DEPTH (m)	BASE RESISTIVITY (Ohm-cm)	LARGE VOLTAGE MECHANISM					
			ORDERS OF MAGNITUDE FOR FIT	AVERAGE ERROR (%)	J_o (A/cm^2)	n	ACTIVATION ENERGY (eV)	POSSIBLE CURRENT MECHANISM
JPL 6 (SiN_x)	0.4	2	2.5	.30	2.1 E-11	1.07	0.96	DEPL LAYER RECOMB VIA SHALLOW TRAP
JPL 8-5 (SiN_x)	0.2	2	2.8	.20	1.7 E-11	1.02	1.00	EMITTER RECOMB WITH S = 10^5 to 10^5 cm/sec
JPL 9-1 (SiO_x)	0.2	2	2.8	.19	3.1 E-11	1.06	0.94	DEPL LAYER RECOMB VIA SHALLOW TRAP
JCGS MINP 84-2	0.2	0.2	2.0	.4	1.3 E-12	1.02	1.10	EMITTER RECOMB WITH S = 10^3 to 10^4 cm/sec

depletion layer recombination. The large voltage mechanism for JPL 8-5 is characterized by a n-value close to 1.0 and a value of ϕ which is consistent with bandgap narrowing.[6] Referring to Figure 18, the value of $J_{02} = 1.7 \times 10^{-11}$ A/cm^2 is consistent with a value of $S = 10^5$ to 10^6 cm/sec assuming $N_S \approx 1 \times 10^{20}$ cm^{-3}. Cell JPL 9-1 exhibits properties more consistent with depletion layer recombination.

Results have been included for the JCGS MINP cell 84-2 for several reasons First, note that the large voltage characteristics can be interpreted in terms of emitter recombination assuming $S = 10^3$ to 10^4 cm/sec. (See Figure 18) This value of surface recombination velocity is consistent with the value deduced from photoresponse. It should be noted that the base region contribution to J_0 for a 0.2 Ohm-cm base is $\approx 3 \times 10^{-13}$ A/cm^2. Thus, with a 0.2 Ohm-cm base, it is possible to observe results of achieving low values of S. In future studies, we will request cells from JPL that are fabricated on 0.2 Ohm-cm base material. It is also probably desirable to utilize FZ material since the CZ material may have relatively high concentrations of defects which can cause depletion region recombination.

Illuminated characteristics of the shallow junction JPL cells are summarized in Table 8. Results for the SiO_x coated cells are also included. The short circuit current values exhibited by the cells coated with SiN_x were similar to those having SiO_x AR layers. The SiO_x coated cells had slightly larger values of fill factors and V_{oc} than the SiN_x cells, apparently due to lower values of S on the SiO_x coated surfaces. Higher quality SiN_x films like those achieved on the JPL cells with deep junctions should yield improved efficiencies and V_{oc} values.

TABLE 8

ILLUMINATED CHARACTERISTICS OF JPL CELLS (FABRICATED BY ASEC)

CELL	ORIENTATION	AR LAYER	AM1* EFFICIENCY (%)	I_{sc} (mA)	V_{oc} (mV)	FF	TOTAL AREA J_{sc} (mA/cm^2)
2-3	(100)	SiO_x	15.2	130	583	.798	32.6
4-1	(100)	SiO_x	14.7	129	579	.786	32.3
1-5	(100)	SiN_x	14.6	130	570	.793	32.7
2-6	(100)	SiN_x	14.7	130	571	.791	32.7
9-1	(111)	SiO_x	15.0	130	581	.795	32.5
10-2	(111)	SiO_x	15.7	134	588	.796	33.5
8-5	(111)	SiN_x	14.4	128	570	.786	32.0
9-2	(111)	SiN_x	14.8	130	573	.792	32.8

*EFFICIENCY MEASURED AT JCGS WITH ELH SIMILATOR. THE SIMULATOR HAS BEEN CALIBRATED BY EXCHANGING A REFERENCE CELL WITH SERI.

7. GATED DIODE DEVICE STUDIES

Efforts were devoted to preliminary studies of the use of experiments with gated diode structures for characterization of surface recombination phenomena. It is particularly desirable to utilize essentially a solar cell structure for the measurement.

Figure 21 describes an approach to measuring S based on the Rosier method.[7] By controlling the surface potential one can vary the value of S to show whether or not a cell is surface sensitive. If the cell is surface sensitive, then variation of the surface potential would provide additional data and may allow determination of S.

We have carried out preliminary studies on a structure similar to that depicted in Figure 21. To date, if the collector grid contacting the emitter is allowed to be under the gate (separated by a SiN_x layer), the SiN_x layer breaks down between the gate and grid lines at voltages less than one volt. Breakdown was avoided by fabricating a device with the collector grid outside the gate region.

To determine if surface sensitivity could be observed, a 0.2 Ohm-cm silicon substrate with a diffused N+/P junction on the polished surface and an ohmic back contact was used. A Mg tunneling contact was used for a collector in the form of a ring ≈ 1 cm in diameter. SiN_x was deposited over central region. A thin copper film 100 Å thick was then deposited over the central region. We were able to bias the gate ±25 Volts with respect to the emitter and experienced no breakdown.

I vs V_{pn} was measured for -25 Volts < V_{GN} < +25 Volts. A significant change was observed in the low voltage mechanism but no change was observed in the large voltage mechanism. Further work is required before these results can be interpreted.

Photoresponse measurements were also made on this same structure. The thin layer of copper was used for the gate so that photoresponse measurements could be made. Figure 22 shows results for the external photoresponse of the gated diode structure described above. Results are shown for V_{GN} = 0

SURFACE RECOMBINATION VELOCITY — ROSIER METHOD

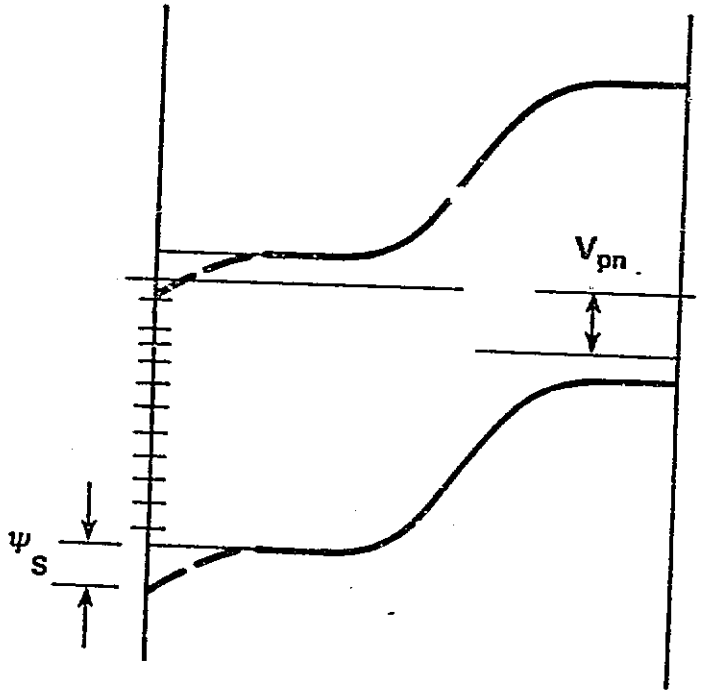

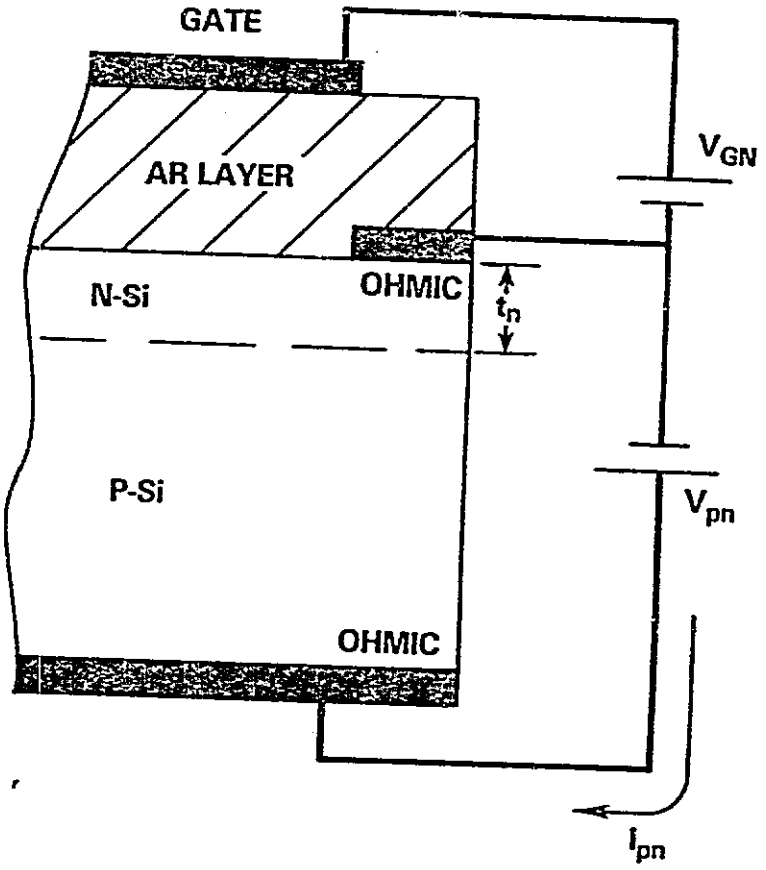

- BASED ON SOLAR CELL STRUCTURE
- ASSUMING $L_p >> t_n$, THE INJECTION CURRENT

$$I_{pn} = \left(\frac{eA_G n_i^2}{N_D}\right)\left(\frac{S}{1+\frac{St_n}{D_p}}\right)\exp\left(\frac{V_{pn}}{kT}\right)$$

- IF CURRENT SENSITIVE TO V_{GN}, THEN:
  - —INJECTION CURRENT DOMINANT AND SENSITIVE TO S
  - —IF KNOW N_D AND n_i^2, CAN DETERMINE S

Figure 21

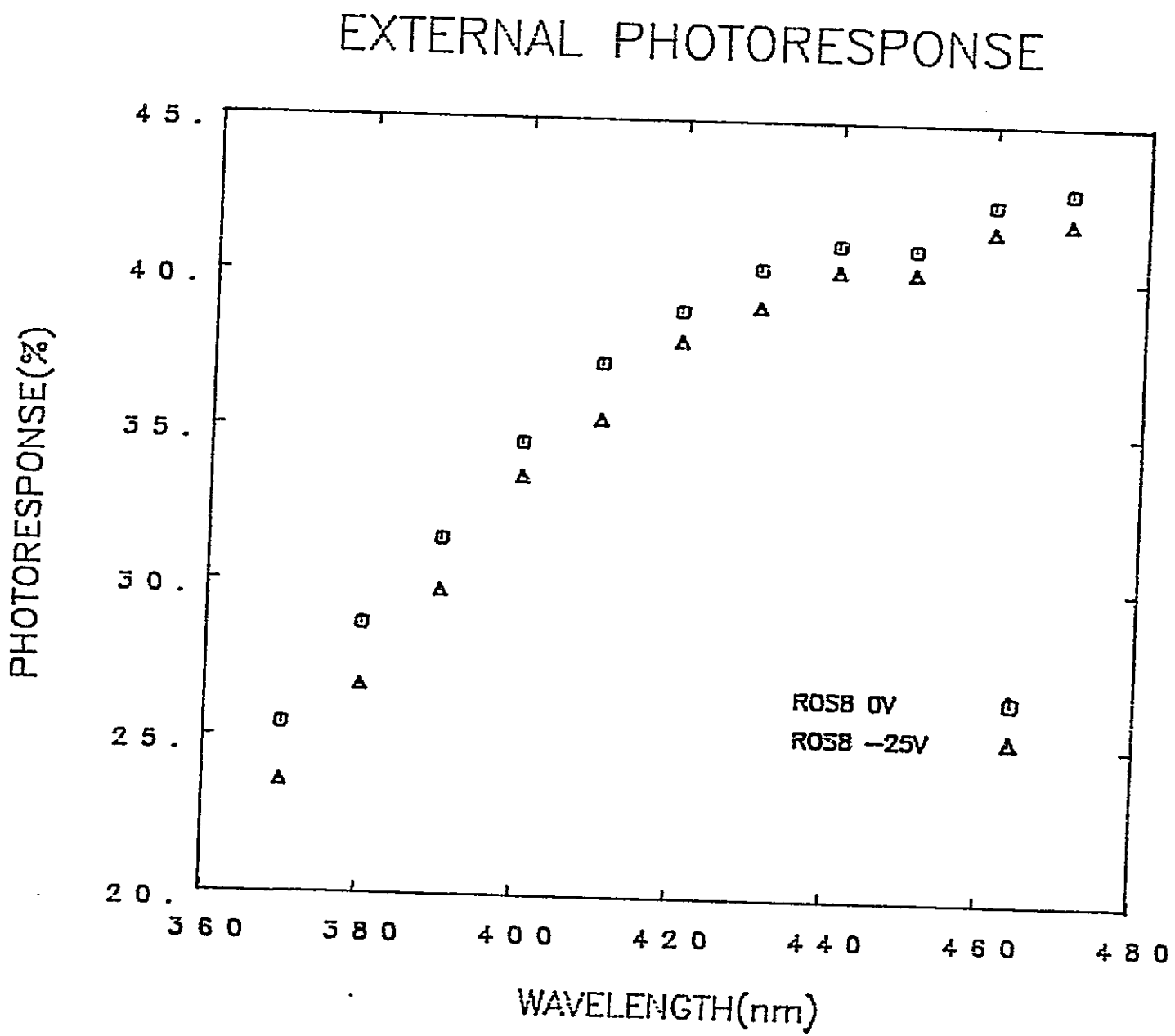

Figure 22. External Photoresponse for Gated Diode Device Showing Decrease In Photoresponse When Gate is At -25 V.

and V_{GN} = -25 Volts. The polarity of V_{GN} is such that the electron bands would move upward (referring to Figure 21), causing an increase in surface recombination losses. As shown in Figure 22, the external photoresponse is reduced by 10 to 15%. No detailed analysis has been carried out. This result simply indicates that photoresponse of a gated diode structure could be useful for investigating surface recombination effects.

8. CONCLUSIONS

One of the main objectives of this program has been to investigate the possibilities for PECVD SiN_x to be effective for passivating the surface of silicon solar cells. In particular, we wish to know whether or not silicon nitride deposited by the low temperature PECVD process yields values of $S < 10^4$ cm/sec on the N^+ surface of high efficiency N^+/P solar cells. The investigations reported here indicate that there is a strong possibility that such values of S can be achieved, but it has not been demonstrated.

Photoresponse studies carried out on N+/P cells provided by JPL indicate that a value of 2×10^4 cm/sec was achieved for the surface recombination velocity. It is expected that with further improvement in the PECVD system, lower values of S may be possible.

Current-voltage analyses provided valuable information concerning selection of cells for future studies. In particular, as a result of our I-V analyses and analytical studies, it is desirable to investigate cells in the future which have the following features:

(i) Low resistivity base material so that reduction of S below 10^4 can be observed--say 0.2 Ohm-cm material;

(ii) Float zone material to reduce the probability for production of traps in the depletion region during cell processing, therefore decreasing the magnitude of depletion region recombination.

(iii) shallow junction on the order of 0.2 μm to insure that minority carrier diffusion in the emitter does not dictate the I-V characteristics.

It will also be desirable to deposit SiN_x onto the front silicon surface before the collector grid is deposited. In all studies carried out on JPL cells, the SiN_x was deposited onto a surface with a Ti/Ag grid. The plasma could have caused some Ti or Ag to contaminate the surface.

Finally, preliminary results with gated diode structures indicate that further investigation of these devices is warranted.

9. FUTURE WORK

Future efforts will involve further studies of approaches to achieve low values of surface recombination velocity. However, these studies will be integrated as part of a larger program to investigate high efficiency silicon solar cells. The program will focus on investigations of silicon cells based on a MINP structure using Mg or Ti tunneling contacts (see Figure 23). The program will involve the following areas of investigation:

(i) Photocurrent--A double Ar coating will be developed along with a capability to limit the grid shadowing to 3.3% so that >36 mA/cm^2 can be achieved.

(ii) Current Losses--Investigations of current loss mechanisms will continue so that a base limited cell operation can be achieved. This achievement would lead to value of V_{OC} and FF necessary for cell efficiencies >20%.

The increase of photocurrent will involve the development of a double AR coating based on TiO_2 and MgF_2. Eventually, it will be desirable to investigate methods for improving carrier lifetime so that values of J_{PH} significantly greater than 36 mA/cm^2 can be achieved.

Reduction of surface recombination velocity on the N^+ surface of N^+/P cells will be a key part of efforts to limit current losses. The use of PECVD SiN_x will continue to be examined for surface passivation, along with the use of a thin thermal oxide. Efforts will initially concentrate on cells based on 0.2 Ohm-cm material, and a cell structure involving a 0.2 μm junction depth, cell thickness of 15 mils, and an ohmic back contact. The donor profile will eventually be tailored to minimize recombination losses in the emitter. Once base limited operation is achieved with this structure, a passivated back surface will be introduced along with a thinner cell thickness. Figure 24 indicates the expected improvements and possible cell performance. See References 8 and 9 for further details concerning work by JCGS on MINP cells, and for further discussion of projected performance of such solar cells.

MINP CELL CONCEPT

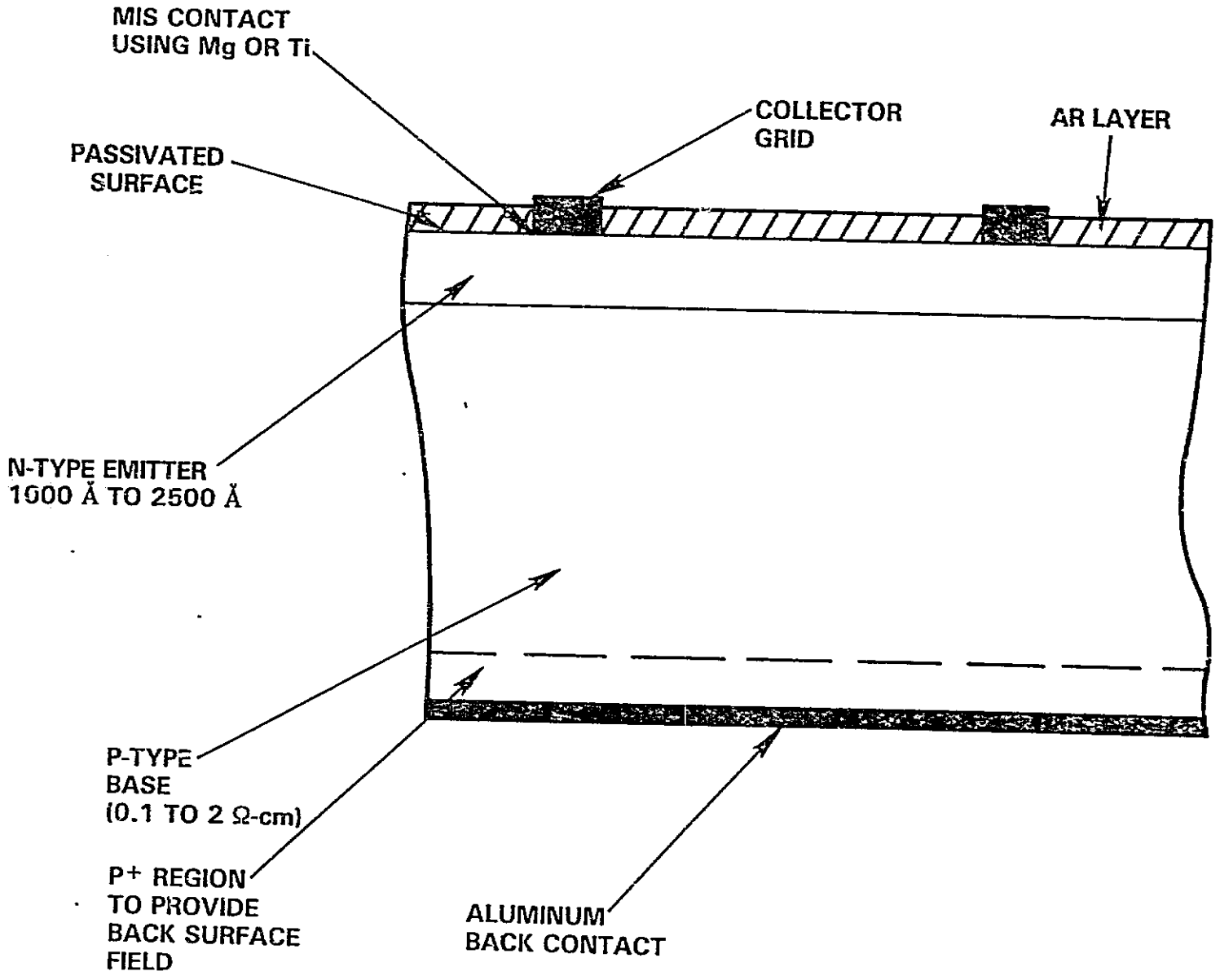

Figure 23

PROJECTED PERFORMANCE

TO ACHIEVE 20%

- MUST REDUCE J_{OE} BY DECREASING N_S AND S_p
- NEED SLIGHT IMPROVEMENT IN L

TO ACHIEVE 25%

- NEED F&P DIFFUSION LENGTH
- MUST REDUCE S_p TO 10^2
- WITH THESE VALUES OF L AND S_p, J_o WILL BE DECREASED TO $\cong 3 \times 10^{-14}$ A/cm²
- MUST USE DOUBLE AR WITH TEXTURED SURFACE OR WITH COMPLETE OPTICAL CONFINEMENT

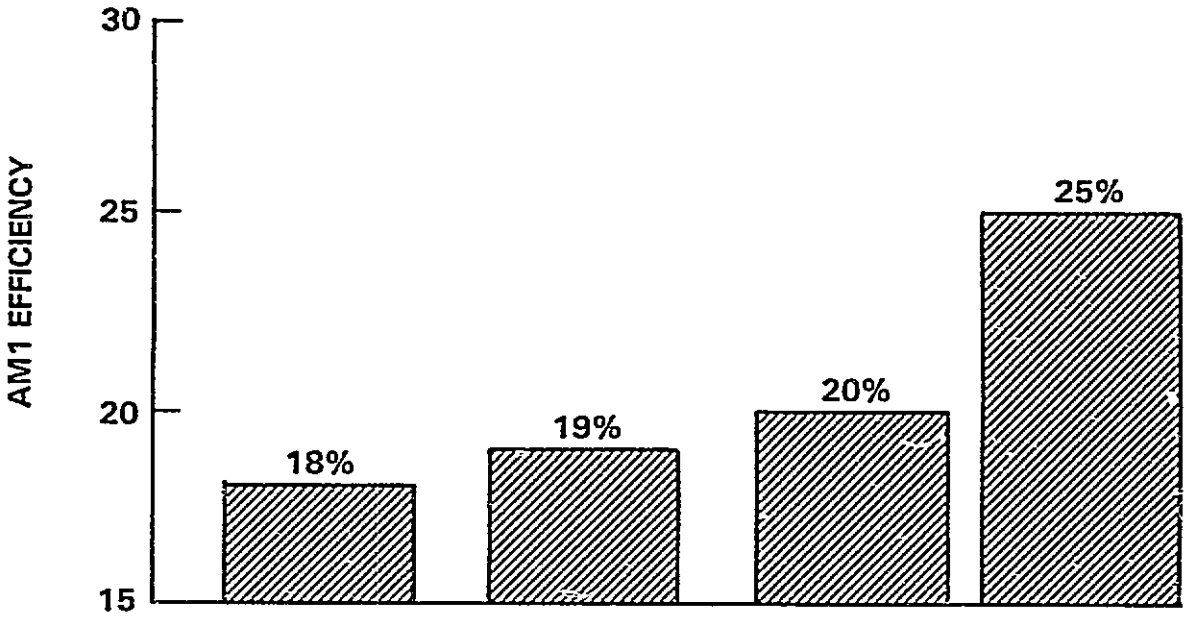

J_{SC}(mA/cm²)	36.0	36.0	36.7	40.9
V_{OC}(mV)	630	650	670	720
FF	.794	:812	.820	.850
J_o(A/cm²)	1×10^{-12}	4.5×10^{-13}	2×10^{-13}	3×10^{-14}
n-VALUE	1.0	1.0	1.0	1.0
N_S(cm^{-3})	6×10^{19}	4×10^{19}	2×10^{19}	2×10^{19}
SURF REC VEL	10^4	10^3	10^3	10^2
DIFF LENGTH	150	150	200	500 (F&P)
GRID SHADOW	4%	4%	3%	2%
CELL THICKNESS	15 mils	15 mils	15 mils	10 mils
BACK SURF	Ohmic	Ohmic	BSF	BSF

Figure 24. Projected Performance Based On Approach To Increase Both J_{sc} and V_{oc}.

REFERENCES

1. G. E. Jellison, Jr. and F. A. Modine, "Optical Constants for Silicon at 300 ^{o}K and 10 ^{o}K Determined from 1.64 to 4.73 eV by Ellipsometry," ORNL/TM-8002, February, 1982.

2. R. Hezel, K. Blumenstock and R. Schorner, "Interface States and Fixed Charges in MNOS Structures With APCVD and Plasma Silicon Nitride," J. Electrochem. Soc. 131, 1679 (1984).

3. M. A. Green, et al., "Towards a 20% Efficient Silicon Solar Cell," Conf. Record 17th IEEE Photovoltaic Specialists Conf., Orlando, May 1984, pages 386-389.

4. C. T. Sah, R. Noyce and W. Shockley, "Carrier Generation and Recombination in p-n Junctions and p-n Junction Characteristics," Proc. IRE, page 1956 (1957).

5. Jerry G. Fossum and M. Ayman, "An Analytic Model for Minority Carrier Transport in Heavily Doped Regions of Silicon Devices," IEEE Trans On Electron Devices ED-28, 1018 (1980).

6. H. P. D. Lanyon and Richard Tuft, "Bandgap Narrowing in Moderately to Heavily Doped Silicon," IEEE Trans On Electron Devices ED-26, 1014 (1979).

7. Laurence L. Rosier, "Surface State and Surface Recombination Velocity Characteristics of Si-SiO_2 Interfaces," IEEE Trans On Electron Devices ED-13, 260 (1966).

8. L. C. Olsen, et al., "High Efficiency Silicon MINP Solar Cells," Conf. Record 17th IEEE Photovoltaic Specialists Conf., Orlando, May 1984, pages 403-408.

9. L. C. Olsen, et al., "Silicon MINP Solar Cells," High-Efficiency Crystalline Silicon Solar Cells Research Forum, Phoenix, Arizona, July 9, 1984 (Proceedings to be published by JPL).